



ELSEVIER

Contents lists available at ScienceDirect

Engineering Failure Analysis

journal homepage: www.elsevier.com/locate/engfailanal

Micro-mechanisms of the ductile-to-brittle transition in hydrogenated zirconium alloys: A review and a comparison analysis of experimental data and theoretical approaches

Mikhail Kolesnik

Karlsruhe Institute of Technology, Karlsruhe, Germany

ARTICLE INFO

Keywords:

Hydride embrittlement
Ductile-to-brittle transition
Fracture
Hydrides
Zirconium alloys

ABSTRACT

The primary objective of this article is to gather comprehensive experimental and theoretical data on the fracture process of hydrogenated zirconium alloys at micro- and nano- levels and conduct an extensive analysis to identify consensus statements and any potential contradictions. The article focuses on the physical mechanisms that contribute to the ductile-to-brittle transition in fracture mode and examines published hypothesis that explain these mechanisms. The manuscript contains a comprehensive list of published experimental studies on the mechanical properties of hydrogenated zirconium alloys. This study will be useful for developing and verifying models and for planning of experimental studies and analyzing their results.

1. Introduction

Metals may absorb hydrogen during its operation due to interaction with the ambient environment in various industrial applications (e.g. as a secondary product of waterside corrosion). Hydrogen embrittlement in steel tubes is evident during the operation of oil and gas pipelines, boiling evaporators at thermal power stations *etc.* [1]. In the nuclear industry, hydrogen embrittlement of zirconium fuel rod cladding and guide tubes in fuel assemblies pose a risk to safe operation, handling and storage after the operation of nuclear fuel for water-cooled nuclear power plants [2]. Hydrogen presence can significantly reduce ductility in steels and zirconium alloys, leading to a transition from ductile to brittle fracture mode, which poses operational risks. This transition, known as ductile-to-brittle transition (DBT), is characterized by temperature, hydrogen concentration, hydride configuration, stress, loading scheme, and loading type. DBT refers to the critical degradation of mechanical properties and should be taken into account when justifying the reliability of operational conditions.

Currently, there is no theoretical model predicting the parameters of DBT in zirconium alloys, nor is there a consensus

Abbreviations: AHL, accumulated hydride length; CPFEM, crystal plasticity finite element method; CTOD, crack tip opening displacement; CZM, cohesive zone model; DBT, ductile-to-brittle transition; DBTT, ductile-to-brittle transition temperature; DDP, discrete dislocation plasticity; DDD, discrete dislocation dynamics; DHC, delayed hydride cracking; EBSD, electron backscatter diffraction; EDC, expansion due to compression (mechanical test); ETEM, environmental transmission electron microscope; FCC, face-centered cubic (crystal lattice); FEM, finite element method; GTN, Gurson-Tvergaard-Needleman (model); HCC, hydride continuity coefficient; HCP, hexagonal close-packed (crystal lattice); HEDE, hydrogen enhanced decohesion; HELP, hydrogen enhanced localized plasticity; HRR, Hutchinson-Rice-Rosengren (model); MD, molecular dynamics (simulation method); PST, plane-strain tensile (mechanical test); RHCP, radial hydride continuous path; RIA, reactivity-initiated accident; RXA, recrystallized annealed (Zircaloy-4); SEM, scanning electron microscopy; SIF, stress intensity factor; SRA, stress-relieved annealed (Zircaloy-4); TEM, transmission electron microscopy.

<https://doi.org/10.1016/j.engfailanal.2024.108110>

Received 23 September 2023; Received in revised form 3 February 2024; Accepted 7 February 2024

Available online 20 February 2024

1350-6307/Â© 2024 The Author(s). Published by Elsevier Ltd. This is an open access article under the CC BY license (<http://creativecommons.org/licenses/by/4.0/>).

understanding of the governing physical mechanism. This article aims to reveal this mechanism analyzing published data on fracture features typical for hydrogenated zirconium alloys at the micro-level in ductile and brittle modes of fracture. A similar approach allowed Djukic [1] to develop a model of ductile-to-brittle transition in steels. However, fracture mechanisms at the microlevel vary across different alloys: atomic hydrogen plays an important role in steels [1] in the processes of hydrogen enhanced localized plasticity (HELP) and decohesion (HEDE), whereas in zirconium alloys, hydrogen solubility is low and the main effect is embrittlement due to hydride precipitation (hydride embrittlement). Therefore, a model of hydrogen embrittlement, developed for steels, which is currently more detailed, cannot be applied for simulating hydride embrittlement of zirconium alloys and *vice versa*.

Zirconium-based alloys exhibit specific features of hydride embrittlement which are related to the tendency of zirconium hydrides to form a network. Hydrides precipitate in zirconium alloys as a platelike dendrites (for example, synchrotron X-ray tomography data on Figs. 5 and 12 in [3]), and can be characterized by their length, thickness, orientation, spacing, and volume density. At high enough hydrogen content level (~ 50 ppm in hydride phase) hydrides form a branched network. The network of hydrides can be determined by its connectivity, which is a combination of parameters mentioned above. Another property of a highly-connected hydride network is percolation, which refers to the ability to provide a hydride-only track through the sample. The parameters of the hydride network affect the fracture process of hydrogenated zirconium alloys. Moreover, the percolation of the hydride network is a necessary condition for hydride-induced DBT in zirconium alloys.

The mechanical properties of hydrogenated zirconium alloys have been extensively researched for several decades, as evidence by numerous studies and reviews [2–11]. However, these researches have not yet comprehensively reviewed and analysed fracture mechanisms at the micro-level. This may have hindered the development of a DBT model for hydrogenated zirconium alloys. Furthermore, certain publications present conflicting interpretations of experimental findings, which have not yet been discussed in literature. There are also instances of theoretical and numerical models that are oversimplified or based on incorrect assumptions published in peer-reviewed journals. Hence, a thorough compilation and portrayal of all existing empirical evidence concerning the fracture of hydrogenated zirconium alloys and their comparison with published models, as well as amongst themselves, is necessary.

This article aims to summarize all published data regarding the mechanical properties of hydrogenated zirconium alloys at a micro- and nano-levels. Section 2 includes experimental data review. Section 3 outlines theoretical and computational models of fracture and DBT, categorized by the specific problem and methodology applied. Section 4 Discussion concentrates on comparing data and providing a phenomenological account to the physical mechanisms at micro-level that result in DBT. Section 5 presents the most comprehensive list of published mechanical tests conducted on hydrogenated zirconium alloys. The list is in the open access and will be updated as new experiments are published. The final Section 6 is conclusion.

2. Experimental data regarding fracture mechanisms at micro- and nano- levels

2.1. Fracture of as-manufactured zirconium alloys

As-manufactured zirconium alloys exhibit ductile fracture with dimples on the fracture surface during tension tests at both room and elevated temperatures, for example [12–14]. The ductile fracture process includes three stages [12,13]: void nucleation, growth due to the plastic deformation of the ambient metal matrix and void coalescence, ultimately leading to the final fracture.

At the fracture of low-alloy Zr-702 (Zr-0.06Ni-0.78(Ni + Fe)-1.2Sn) under room temperature, the first generation of voids nucleate at triple points, as shown in Fig. 1a (data from [15]). The second generation of voids, which appears at higher plastic strains, arises at $Zr_2(Ni,Fe)$ and $Zr(Cr,Fe)_2$ precipitates as well, but voids at triple point remain in the majority [15]. In contrast, in industrial alloys such as as-manufactured Zircaloy-4, nucleation of voids at Laves phase particles $Zr(Cr,Fe)_2$ predominates at room temperature. It has been documented by direct observations of Laves phase presence in the center of dimples at fracture surface, as shown in Fig. 1b here and Fig. 12b in Bertolino [16]. Damage nucleation is mainly due to debonding at the particle/matrix interface (with no evidence of inclusion fracture) [12,16]. Cockeram [17] identified four types of void nucleation sites Zircaloy-2 and Zircaloy-4: (1) slipband

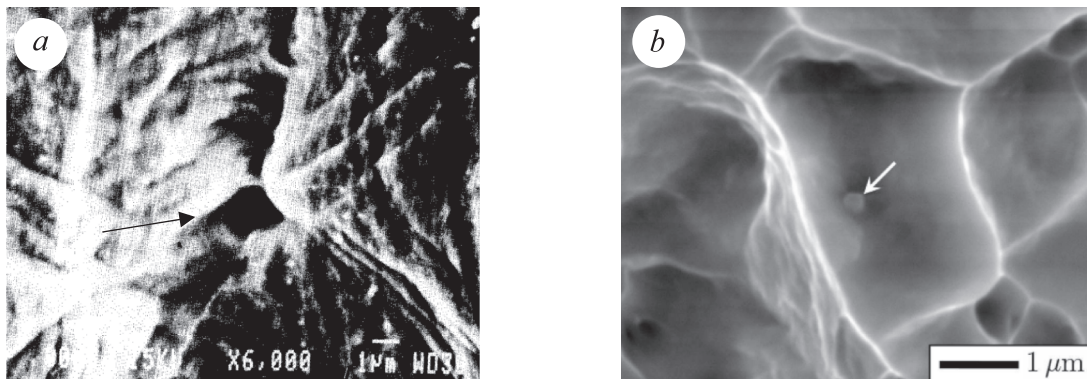


Fig. 1. Main damage nucleation sites in as-manufactured zirconium alloys. (a) at triple node, data by Caré [15], (b) – at inclusions of Laves phase (inclusions at the center of dimples in fracture surface), data by Le Saux [12].

decohesion, (2) intersecting slipbands, (3) impinging slip on grain or lath boundaries and (4) grain boundary or lath boundary intermetallic particles. According to Cockeram [14] and [17], all four mechanisms are presented in α -annealed alloys, whereas nucleation at Laves phases situated along lath boundaries is prevalent in β -treated. The specific microstructure of β -treated Zircaloy-4 consist of colonies of alpha-Zr lath grains with an acicular shape that are contained within prior beta grains, according to [14].

Texture and temperature are two main factors that affect the void nucleation. Texture affects the damage nucleation through at least two mechanisms. Firstly, it is related to anisotropy of properties, which leads to a voids' density in Zr-702 under tension in the rolling direction, about twice as high as under tension in the transverse direction [15]. Secondly, it is caused by density of nucleation sites, which means that the voids density is lower in coarse-grained samples compared to fine-grained [15]. Another factor that affects damage nucleation is temperature. The density of voids, which appear as dimples on the fracture surface, is approximately 15 % lower at 350 and 480 °C than at 25 °C, as can be seen in Table 1 in [12].

Voids growth and coalescence mode are impacted by the local stress state. Zouari [18] investigated the phenomenon through conducting experiments with Zircaloy-4 tubes loaded from inside (expansion due to compression, or EDC test). The study showed a non-monotonic relationship between fracture hoop strain and load biaxiality. Specifically, as the load biaxiality increased from -0.2 to 0.04 , the fracture hoop strain decreased significantly from 0.316 to 0.095 . However, as the biaxiality increased further from 0.04 to 0.75 , the fracture hoop strain then recovered smoothly to 0.137 . This is due to the different mechanisms of void coalescence leading to ductile fracture: at low biaxialities, coalescence occurs via void shearing, whereas at high biaxialities it occurs via internal necking [18]. When necking occurs, the void growth sharply accelerates due to an increase of triaxiality [12,18]. The majority of voids beneath the fracture surface are almost spherical and coalescence occurs due to internal necking of the intervold ligament under axial tension, hoop tension and EDC [12]. However, for plane-strain tensile (PST) tests, the coalescence of voids is primarily caused by internal shearing between voids, although internal necking was also observed [12]. Typically, the fracture surface of unhydrided samples in EDC and PST loadings exhibits different features, while the macroscopic fracture mode remains the same for both (through-thickness slant ductile fracture) [12].

2.2. Effect of hydrogen on the fracture mechanism of zirconium alloys

At low concentrations (several ppm at room temperature), hydrogen is present in zirconium alloys as a solid solution. Atomic hydrogen dissolved in the metal matrix increases the mobility of the dislocations and hence the creep rate and ductility of the metal, as reported in [19] and [20]. This effect is known as hydrogen-enhanced localized plasticity (HELP) mechanism, and was also observed by Fagnoni [21,22]. According to experimental data by Le Saux [12] and Jung [23] the material mechanical strength declines as the hydrogen concentration in solid solution increases, but it rises as hydrogen concentration in hydride phase increases. TEM observations confirmed the increase in screw dislocation mobility with the presence of dissolved atoms of hydrogen in HCP α -Ti, [24]. Recently, *in-situ* ETEM experiments conducted by Huang [25] in bcc α -iron, clearly demonstrated the enhancement of the screw dislocation motion due to the effect of dissolved hydrogen atoms. Domain [26] provided a possible explanation of this effect in Zr-H system through *ab initio* calculations based on density functional theory. They showed that hydrogen atoms reduce stacking fault excess energies, thus enhancing planar slip and hindering cross-slip.

As the hydrogen concentration increases, and hydrides begin to precipitate, the fracture mechanisms undergo gradual changes. For example, according to Bertolino [16], the density of Laves phase particles on the fracture surface of Zircaloy-4 at room temperature smoothly grow with increasing hydrogen concentration up to 250 – 350 ppm. Presumably, Laves phase particles situated at grain boundaries act as preferred nucleation sites for hydrides, resulting in multiple inhomogeneities that cause local embrittlement of the sample [16]. Another hypothesis is that Laves phase particles absorb hydrogen and expand, producing local stress concentrators [12].

At higher hydrogen concentrations (above ~ 350 ppm for Zircaloy-4 at room temperature) the impact of Laves phase particles decreases, indicating that the hydride phase begins to dominate the processes of damage nucleation and crack growth for both ductile and brittle macroscopic fracture modes [16]. Hydrides precipitate as platelike dendrites, primarily in FCC δ -phase $ZrH_{1.6}$ (at

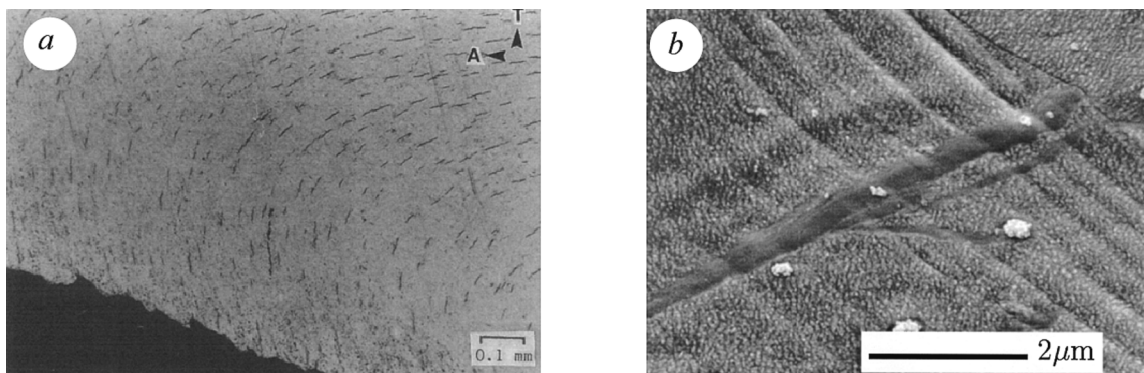


Fig. 2. Evidences for plastic behavior of hydrides: (a) – plastic flow-induced hydride reorientation at 200 °C, data by Choubey [27]; (b) – continuity of slip between the Zr matrix and hydride, data by Grange [36].

conditions, typical for practical applications) [2]. In highly hydrogenated samples the damage nucleates almost only on fractured hydrides, at least at low temperatures [12].

However, hydrides can exhibit basic plasticity even at room temperature, which increases at higher temperatures. The ability of hydrides to undergo plastic deformation together with the metal matrix is demonstrated by the plastic flow-induced reorientation of hydrides in some samples subjected to fracture tests, as shown in Fig. 2a. Evidences that hydrides plastically reorient along the external tension direction near the fracture surface is available in Choubey [27] or Arsene [28], and that they become longer and thinner maintaining their integrity during plastic deformation, reported by Huang [29]. Moreover, scanning electron microscopy (SEM) *in-situ* test has confirmed that slip bands from the metal slip system can pass through the metal/hydride interface, as can be seen in Fig. 2b here, Fig. 9 in Li [30], and Fig. 2 in Arsene [31]. Micropillar compression experiments conducted by Weekes [32] also confirmed that slip bands initiated in the metal matrix can cross the hydride/matrix interface, although not always, and may be terminated by the hydride surface as well. The nanoindentation tests carried out by Puls [33], and Wang [34] have also shown ductile behavior of zirconium hydrides. Lastly, Kerr [35] had found that the creep of the hydride phase controls the slope of the applied stress versus lattice strain curve at stresses above the metal yield in hydrogenated Zircaloy-2 (~ 90 ppm) at room temperature, using the *in-situ* synchrotron X-ray diffraction method.

Hydrides fracture in a brittle manner if the plastic strain surpasses the threshold value, at least at low temperatures. Li [30] observed the initiation of a crack in hydrides *in-situ* in fatigue test at room temperature after 5000 loading cycles by SEM. Besides, brittle fracture of individual bulk hydrides was detected as an acoustic signal in acoustic emission tests [27,37,38,39]. The plastic strain threshold for sample fractured due to hydrides is strongly influenced by load triaxiality. In Zr-2.5Nb at room temperature, the threshold was $\sim 5\%$ under uniaxial and $\sim 1\%$ under triaxial stress state [38]. Simpson [39] confirmed that the threshold strain decreases with increasing triaxiality in tests with smooth and notched samples. The threshold strain decreases also as the metal yield stress decreases: in reactor grade zirconium the equivalent plastic strain is only 0.2% [37]. Surface hydrides exhibit qualitatively comparable, albeit quantitatively diverse behavior in comparison with bulk hydrides. SEM *in-situ* data at room temperatures indicate that surface hydrides fracture at equivalent plastic strain above 20% in Zircaloy-2, according to Yunchang [40], and at $15 - 25\%$ after necking in Zircaloy-4, according to Grange [36]. Pure zirconium, on the other hand, experience surface hydrides fracture at plastic strain only $\sim 5 - 8\%$, according to Warren [41] (tested at cryogenic temperature -196°C). The fracture threshold of hydrides decreases with a rise in hydrogen content, as it was observed within the range of $400 - 1200$ ppm in Zircaloy-4, according to Fig. 17 in [12] and within the range of $20 - 180$ ppm in Zr-2.5Nb, [39]. Such an effect can be due to the fact that coarse hydrides breaking at lower plastic strain when compared to fine ones. According to Arsene [31], some surface hydrides having the greatest thickness may fracture at a matrix strain around 10% , while others retain their integrity up to strain 50% . However, Puls [38] reports that the critical plastic strain at fracture depends on the average length of hydrides rather than their thickness. Hydrides longer than $\sim 50 - 100\ \mu\text{m}$ fracture with minimal plastic deformation. Besides, Barraclough [42] demonstrated that the fracture stress rises with the volume fraction of γ -phase when mixed ($\delta + \gamma$) hydride phases are present. This can be linked to the resistance offered by γ -platelets to the propagation of cleavage cracks in the δ -phase.

A brittle crack nucleates within hydrides mainly at the intersection of a slip band in the metal and the surface of the hydride, as displayed in Fig. 3 here, according to [31,43] and [44]. Slip bands from zirconium matrix can terminate at the hydride/matrix boundary and cause interfacial shear and cracking in some areas [45]. In general, the slip band can either initiate plastic slip within the hydride or get arrested in the matrix/hydride interphase, depending on the slip direction and the orientation relationship of the metal and the hydride, [46]. If dislocations moving in the metal matrix can't pass through the interphase, they form a pile-up that acts as a local stress concentrator, increasing the risk of the hydride fracture. Dislocation immobilization by interphase boundaries results in significant strain localization and a more heterogeneous deformation field in hydrided zirconium matrix compared to non-hydrided one [45]. Wang [47] observed a considerable increase in the local dislocation density near the hydride/matrix interface due to the pile-up of dislocations in microcantilever bending tests of hydride-free and hydride-containing single crystal of Zircaloy-4. Experiments carried out by Warren [41] at cryogenic temperatures (-196°C) confirm that damage initiates where hydrides are intersected

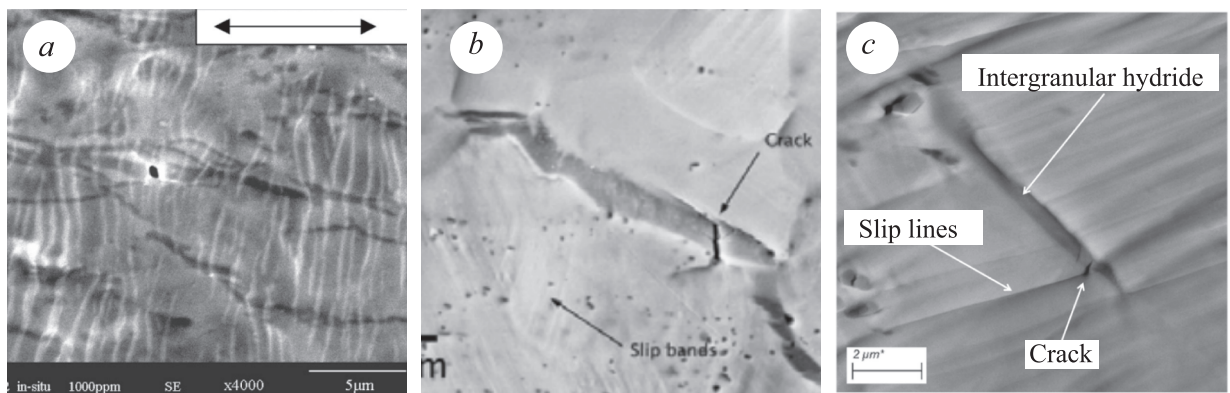


Fig. 3. Evidences of crack nucleation in hydrides at the intersection with a slip band. (a) data by Arsene [31], (b) – hydride at a grain boundary separating a soft and a hard grain, data by Reali [43], (c) – data by Reali [44].

with slip bands and, beyond that, by twins in the zirconium. At room temperature, twins can also cause fracture of hydrides if they intersect with the phase boundary, however, in comparison to slip bands, their effect is negligible, according to experiments by Beevers [48].

EBSD method, applied by Reali [43], has clarified that cracks nucleate primarily on intergranular hydrides between soft and hard grains with the high misorientation. Supporting this find, experimental data by Silva [49] and Grange [36] also confirm the significant role of intergranular hydrides in the damage nucleation process. Intergranular hydrides pose a higher risk of dislocation pile-ups due to the need for slip bands to cross two types of barriers: the interphase and the grain boundary, as opposed to only the interphase boundary for slip band crossing intragranular hydrides.

A brittle crack within a hydride is oriented perpendicular to external tension; for instance, Arsene [31] and Reali [43]. During the fatigue tests of rings subjected to tension carried out by Li [30,50], tangential hydrides (oriented along external tension) cracked in the through-thickness direction, whilst radial hydrides (oriented perpendicular to external tension) cracked along their length direction and at lower critical strain. *In-situ* SEM observations of ring tests reported by Zhang [51] confirm that radial hydrides exhibit brittle fracture along their length and are more preferable for crack nucleation, while longer tangential hydrides maintain their integrity in the vicinity of fractured radial hydrides, as shown in Fig. 4.

The plastic zirconium matrix blunts the brittle crack started within a hydride, as can be seen in Fig. 3a here, Fig. 14 in Grange [36], Fig. 4 in Yunchang [40], Fig. 2 in Arsene [31], Fig. 2 in Kim [52], Fig. 8 in Glendening [53]. Following further plastic deformation, initial transverse cracks of hydrides area are able to open to spherical pores, creating the row of voids, as displayed in Fig. 5 (data by Puls [37] and Le Saux [12]). The shape of pores may be irregular at room temperature, but at higher temperatures, they become more spherical due to the increasing plasticity of the metal. Puls [37] observed that multiple cracks in the hydride may also initiate the growth of deformation pores in the metal matrix, as can be seen in Fig. 1 in [37].

Brittle fracture is fully localized inside hydrides. Besides SEM-evidences about brittle crack nucleation in hydrides given above, it can be confirmed by presence of brittle cleavage areas on the fracture surface of hydrogenated samples demonstrated macroscopically ductile fracture, as shown in Fig. 6 here (data by Gopalan [54]) and Fig. 12a in Hsu [13]. Since cleavage areas are enclosed areas with diameter similar to the length of hydrides, it is suggested that cleavage can only propagate through hydrides, and zirconium ligaments between them undergo ductile fracture. Additionally, Huang [55] report that the coverage percentage of brittle area on the fracture surface increases with increasing hydrogen concentration. Microcantilever tests conducted by Chan [56] confirm that hydrides fracture in a brittle manner, while α -Zr exhibits ductility, at least at room temperature. Further, fatigue cracks tend to propagate along the hydrides, and the hydrides at the front of the cracks can change the fatigue crack propagation path, as reported by Zhang [57]. Finally, secondary brittle cracks that are oriented perpendicular to the fracture surface also grow along hydrides. Secondary cracks may be observed during SEM fractography when large hydrides are present in the sample, as displayed in Fig. 7 a here (data by Chu [58]), Fig. 15 in Le Saux [12], Fig. 11b – 11d in Huang [29], Fig. 9 in Hsu [59], Fig. 14 in Chan [60], Fig. 9 in Min [61], Fig. 10a in Li [50]. Additionally, secondary cracks can be detected near the fracture surface in a transverse direction, as shown in Fig. 7b here (data by Hong [62]) and Fig. 2 in Tomiyasu [63]. The only known exception is fatigue crack growth along slip bands under cycling load, as it was observed after $\sim 10^4$ cycles by Li [30]. However, this type of loading is not conventional for the typical nuclear fuel life cycle, and is only available due to pellet-cladding interaction during regular power manoeuvres.

As temperature increases, the brittleness of hydrides decreases to negligible values. An acoustic emission test shows that the number of brittle fractures of hydrides decreases by an order of magnitude at 200 °C compared to room temperature, as can be seen in Fig. 5 in Choubey [27]. A SEM study by Le Saux [12] revealed that there was no fragmentation of hydrides at 480 °C and very few fractures at 350 °C, while multiple brittle fractures of hydrides were observed at 25 °C. SEM-fractography conducted by Raynaud [64] has confirmed that fracture surfaces of hydrogenated Zircaloy-4 are different at 25, 300 and 375 °C: large brittle primary voids nucleate at large hydrides at room temperature, while at 300 and 375 °C hydrides fracture in ductile mode [64].

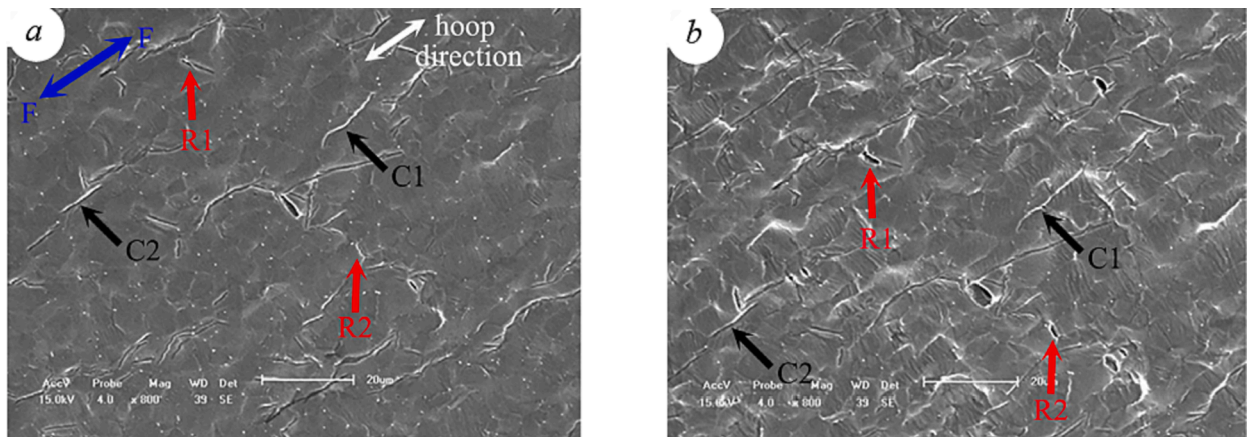


Fig. 4. In-situ SEM observation of the crack initiation and growth along the length of radial hydrides (marked as R1 and R2) at ring tension test; (a) and (b) – displacements 0.80 mm and 0.95 mm, data by Zhang [51].

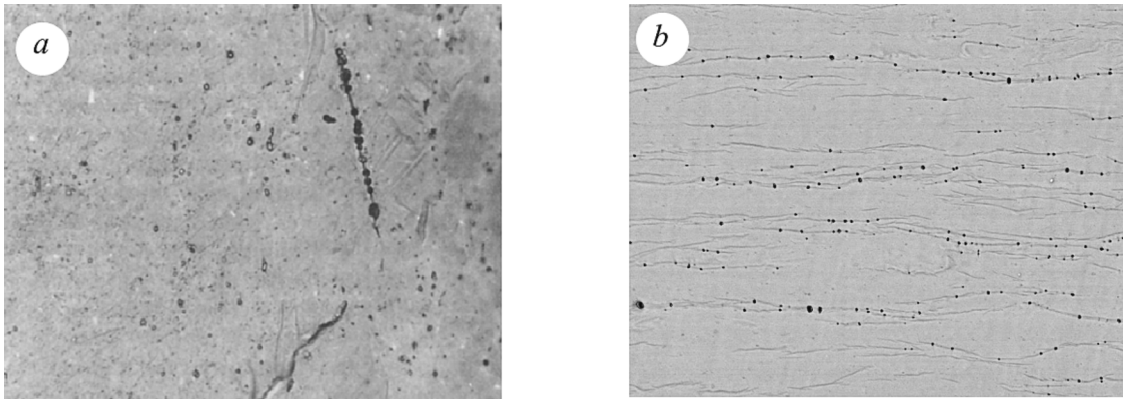


Fig. 5. Row of voids along hydrides, (a) – data by Puls [37], (b) – data by Le Saux [12].

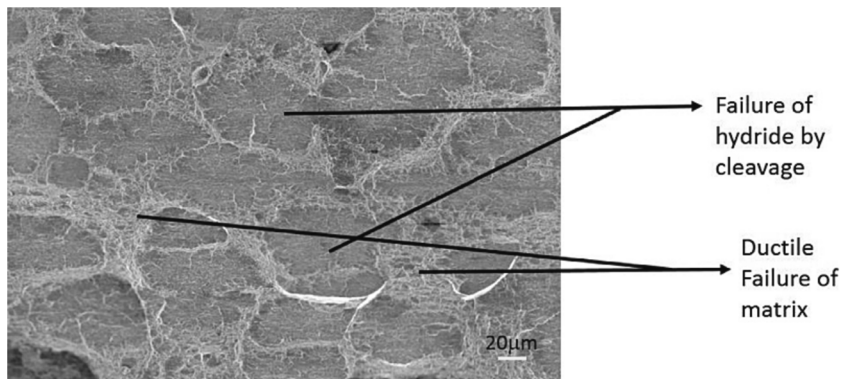


Fig. 6. A brittle fracture is localized inside hydrides, while zirconium fracture is ductile, data by Gopalan [54].

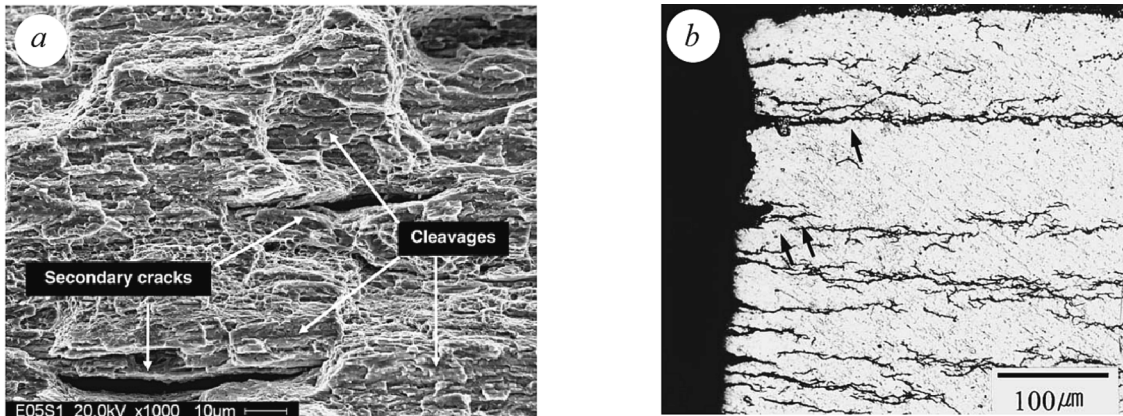


Fig. 7. Secondary cracks perpendicular to fracture surface; (a) – SEM fractography of fracture surface, data by Chu [58], (b) – transverse cross-section, data by Hong [62].

2.3. The balance between ductile and brittle fracture mechanisms in hydrogenated zirconium alloys

Fracture of zirconium alloys can occur through various modes, which are dependent on factors such as hydrogen content, temperature, loading scheme and other parameters. Different research groups apply different classifications to describe failure modes at macro-level. This creates certain difficulties, but is associated with objective reasons, specifically the use of different samples and loading schemes. For example, Kim [52] have observed three fracture modes of macroscopic fracture in ring tests of hydrogenated zirconium alloys (Zircaloy-4, HANA-4, HANA-6): (1) cup-and-cones, (2) 45° shear and (3) brittle (flat). Puls [38] identified four

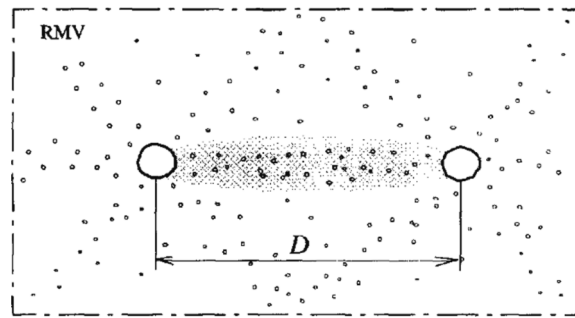


Fig. 8. The scheme of plastic shear localization mechanism: two large voids of the first generation and distributed small voids of second generation. Voids in shaded zone participate in coalescence process in the presence of external tension, data by Faleskog [66].

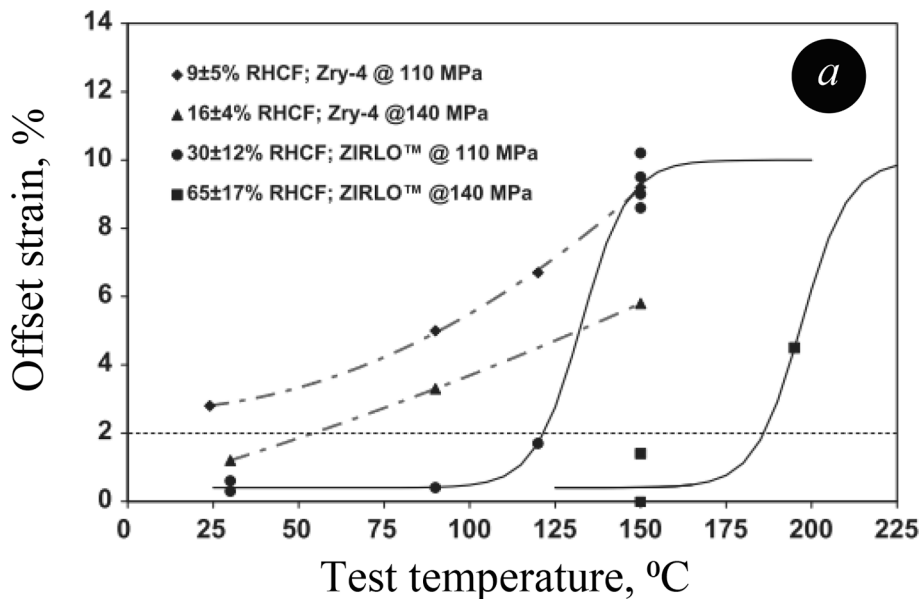


Fig. 9. Ductility versus temperature and DBTT. Each curve is relevant for a specific hydride morphology. (a) – data by Billone [69], (b) – data by Kim [70], (c) – data by Sharma [71].

fracture modes of smooth flattened specimens: (1) diffuse neck and fracture at 90° to the tensile axis, (2) localized neck oriented at 60° to the tensile axis, (3) 60° neck starting from either edge, but then became perpendicular (zigzag) and (4) flat fracture perpendicular to the tensile stress axis. And Le Saux [12] reports the following five fracture modes in tests with different loading schemes: (1) slant, (2) cup-and-cone like, (3) stable, (4) through-thickness slant and (5) flat. Only the last mode in all described above examples represents the brittle fracture, while the others correspond to ductile behavior.

Nevertheless, only a few basic mechanisms present fracture modes at micro-level. Even in the most general case (fracture of metals), brittle fracture result from cleavage or intergranular/interphase decohesion, while ductile fracture occurs due to cavitation or plastic instability, according to Pineau [65]. In the case of hydrogenated zirconium alloys, brittle micromechanisms are only presented by cleavage through hydrides. The only evidence of cracking along the metal/hydride phase boundary was observed by Li [30] under cyclic loading conditions after $\sim 10^4$ cycles (beyond the typical nuclear fuel life cycle conditions). Ductile fracture of hydrogenated zirconium-based alloys occurs mainly through the classical mechanism of voids nucleation, growth, and coalescence. However, significant plastic deformation and necking are often required for cavitation [12,27,43,51]. Alternatively, void coalescence can occur in the plastic instability manner [12].

Compound fracture mechanisms are also possible based on few fundamental micromechanisms listed above. For high-strength metals, Faleskog [66] proposed the plastic shear localization mechanism, which relies on void coalescence in quasi-brittle ductile fracture and has a low fracture toughness. The mechanism presumes two generations of voids: large pores of the first generation and smaller voids of the second one. Further, the inhomogeneous stress field of the large voids results in the rapid growth of small voids between them, which ultimately leads to coalescence, as shown in Fig. 8. Le Saux [12] assumes that this mechanism can occur on microscale for the zigzag type fracture of hydrogenated zirconium alloys, as displayed in Fig. 3 in [12]. According to Le Saux [12], the

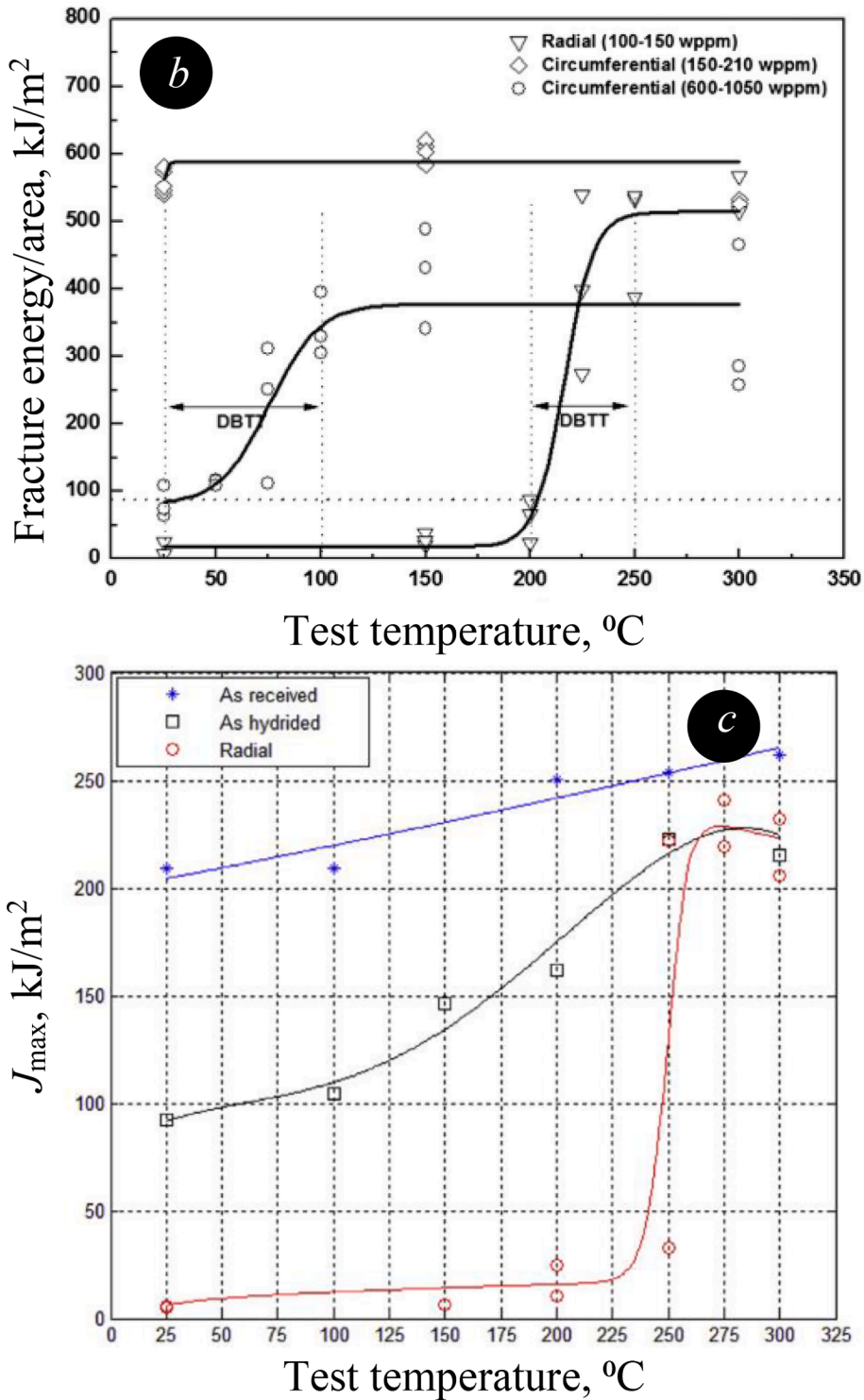


Fig. 9. (continued).

first generation of voids nucleate at fractured hydrides, whilst the second generation nucleates at grain boundaries and Laves phase particles.

The primary external factors, determining the balance between brittle and ductile mechanisms and, therefore, the fracture mode, are temperature, stress level and loading scheme. Meanwhile, the external conditions for DBT depend on the hydrogen concentration, hydride morphology, microstructure, texture and metallurgical state of the alloy.

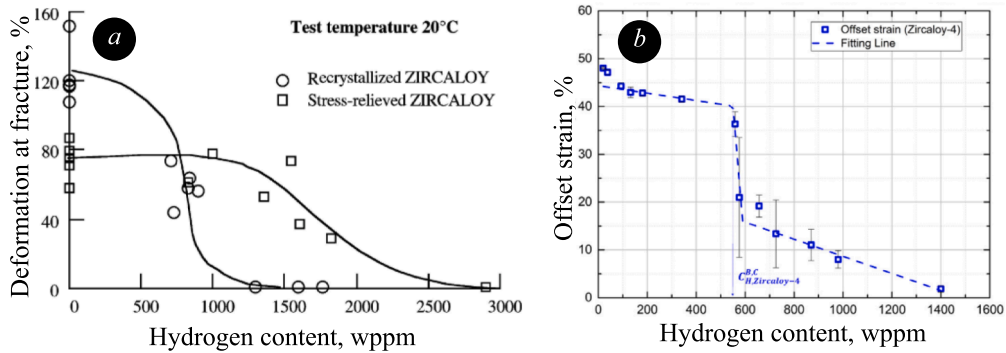


Fig. 10. Zircaloy-4 plasticity versus hydrogen content; (a) – data by Arsene [28], (b) – data by Kim [77].

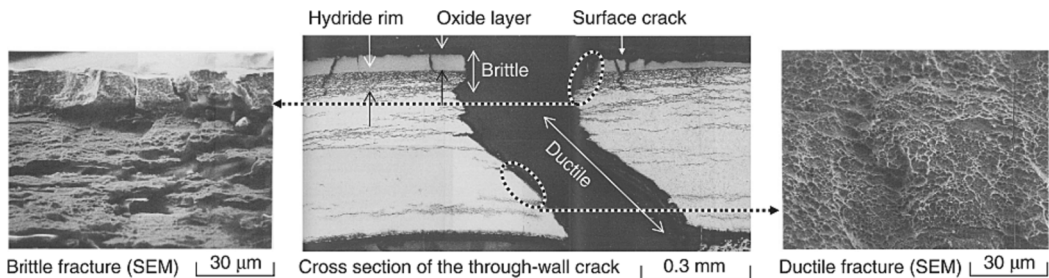


Fig. 11. Fracture of high-burnup fuel cladding with rim; data by Tomiyasu [63].

The temperature is one of the most significant factors influencing the plasticity parameters of the sample, including fracture roughness, offset strain, or others. Even a moderate temperature increase of 50 – 100 °C can cause these parameters to increase by 3 – 10 times, as shown in Fig. 9 here, [67,68,69,70,71,72,73,74]. The DBT in samples with radially-oriented hydrides may be much sharper than in samples with tangentially-oriented hydrides, as can be seen in Fig. 9b and 9c. This difference may be due to a wider temperature interval with a mixed fracture mechanism in samples with tangentially-oriented hydrides, resulting from the hydride network's inability to provide a brittle crack through the sample, which is necessary for a fully brittle crack. According to the fractography analysis, brittle fracture at temperatures below the DBT temperature (DBTT) exhibits a total dominance of cleavage through hydrides as a fracture micro-mechanism. Analogue samples at temperatures above DBTT exhibits either mixed or fully ductile dimple structures of the fracture surface, which indicate micro-void coalescence [12,28,68,70]. As the temperature rises further above DBTT, the ductile fracture enhances its dominance. For instance, Hsu [13] reports that Zircaloy-4 samples containing 250 – 300 ppm of hydrogen experience ductile fracture at both 25 and 300 °C. However, the fracture surface at 25 °C exhibits both quasi-cleavages and dimples, indicating mixed mechanisms at micro-level. In contrast, the fracture surface at 300 °C shows exclusively ductile tearing dimples. At temperatures significantly higher than the DBTT, the fracture toughness is only slightly affected by temperature, hydrogen content and hydride morphology. This is supported by Fig. 9 in this study, as well as Fig. 8 in [59], Fig. 6a in [71], Fig. 5 in [75], Fig. 3 in [73], Fig. 13b in [72]. The fatigue crack growth rates at 300 °C remains nearly constant as the hydrogen content increases, while at room temperature it increases with the increase of hydrogen content, according to data by Zhang [57] (with the same hydrogen content, the fatigue crack growth threshold at 300 C is lower than that at room temperature). The main difference between the as-manufactured and hydrogenated samples at temperatures above DBTT is that the hydrogenated samples exhibits a greater concentration of dimples at fracture surface for 30 – 60 %, as can be seen from Table 1 in [12]. During high-temperature fracture, the role of hydrogen is to create additional nucleation sites of voids due to additional local inhomogeneities because of volume increasing of intermetallics $Zr(Fe,Cr)_2$ absorbing hydrogen, as assumed Le Saux [12], or due to remaining hydrides causing dislocation pile-ups.

The hydrogen concentration in the sample also has a significant impact on mechanical properties and may cause the change of fracture mode, as shown in Fig. 10. As reported by Silva [49], Zircaloy-4 plates fracture in a ductile manner (cup-and-cones mode) at room temperature when the hydrogen content is between 25 and 250 ppm; fracture mode is mixed with isolated areas of cleavage when the hydrogen concentration is within the range 420 – 450 ppm and fully brittle with cleavage dominance above 1230 ppm. Arsene [28] and Bai [76] also observed a fully brittle fracture of Zircaloy-4 when hydrogen concentration is above 1000 ppm and sharp DBT in the range 500 – 1000 ppm; however, Kim [77] provided lower threshold concentrations of DBT: ~ 550 ppm for Zircaloy-4 and ~ 500 ppm for Zr-Nb alloy. On the other hand, Martín-Rengel [78] found that ZIRLO™ alloy exhibit a smooth and gradual dependence (without sharp transition) in ductility as the hydrogen concentration increases up to 2000 ppm, as displayed in Fig. 20 in [78], and even at 2000 ppm the fracture mode is mixed and includes both ductile shearing and quasi-cleavage mechanisms, according to Fig. 11 in [78]. The alteration of fracture mode and DBT due to hydrogen concentration increment arises due to the formation of interlinked

hydride network.

The influence of *hydride rim and blister* on fracture mode provide further evidences of the significance of hydrogen concentration. Strain to failure decreases as the thickness of hydride rim or the depth of blister increases both at room and higher (300 – 480 °C) temperatures [79,53,80,72]. It appears that the rim or blister plays a role in initiating a brittle crack. Fractography indicates that rim fractures occur via brittle mode perpendicular to external tension, even in cases where the material underneath fractures in the ductile mode with a slope 45°, as shown in Fig. 11 here, Fig. 14 in [72], Fig. 9d and 10d in [81]. SEM data obtained by Tomiyasu [63] support the observation that the dominant mechanism involved with rim fracture is cleavage, while the fracture surface of the metal below the rim is covered by ductile dimples present, as displayed in Fig. 14. Notably, the rim and the metal layer situated below it both contain hydrogen in the hydride phase, but in different concentration.

However, the impact of hydrogen concentration on the embrittlement degree is not always monotonic, as shown in Fig. 12. The highest degree of embrittlement is exhibited by specimens with a hydrogen concentration equal to the solubility at the maximum temperature in the preceding thermomechanical treatment (hydride reorientation treatment), Fig. 12b. Daum [82] explains it through hydride morphology factor: the most harmful hydride morphology is generated in samples where hydrides experience complete dissolution and reprecipitation in thermomechanical cycling; more recent evidences supporting this statement is presented in Fig. 6 in [83] and Fig. 4 in [84]. Therefore, it is important to consider both the hydrogen concentration factor and the hydride morphology factor.

The morphology of hydrides is another factor significantly affecting the fracture mechanisms [58,60,82,86,87,88,89,90]. Morphology is understood here as a set of following parameters: orientation, hydride spacing, its length and thickness. Reorientation of hydrides can change fracture mechanisms at both the micro- and macro-levels. Zirconium samples with hydrides oriented perpendicular to external tension are more susceptible to brittle fracture compared to those with hydrides oriented parallel to the tension, even when the hydrogen concentration is equal, according to SEM data in [59,61,71,91,88]. For instance, the complete reorientation of hydrides resulted in a shift of the DBTT from the range of 200 – 250 °C to the range of 25 – 100 °C in a Zircaloy-4 sample with 100 – 200 ppm of hydrogen, as shown in Fig. 9b here (data by Kim [70]). The reorientation also caused a shift in the DBTT of more than 100 °C, according to Fig. 12 in Kim [92]. Additionally, the distance between hydrides plays a crucial role in crack propagation and void coalescence. It determines whether a cracked hydride can cause its neighbour to crack, and at which plastic strain the voids nucleated at neighboring hydrides can coalesce through the metallic ligament between them. According to experimental data reported by Arsene [28], the critical distance between hydrides that restrict the crack growth is 0.5 μm. Thickness and length impact the brittleness of hydrides (large hydrides being more prone to a brittle crack nucleation), as previously mentioned in Section 2.2 with the references to works of Arsene [31] and Puls [38]. Another coupled effect of length and orientation is the creation of a continuous path for brittle crack propagation, requiring less fracture energy than a crack path through the ductile metal. Therefore, the connectivity of a hydride's network determines the hydride embrittlement degree and DBT conditions. Various metrics of connectivity are defined as a combination of hydrides length, orientation and volume density. These metrics exhibit a substantial correlation with the mechanical properties of a hydrogenated zirconium alloy, as evidenced by sources [54,69,75,85,93,94]. For example, Fig. 13 depicts the correlation between ductility and the widely-used metrics in practice, namely hydride continuity coefficient (HCC) or accumulated hydride length (AHL) [54,75,85,93]. Both metrics are defined as a summary of the hydride length projection on a direction perpendicular to external tension, which is then normalized to the sample's width. Furthermore, other factors, such as grain size, hydride rim-layer, texture, and metallurgical state (which will be discussed below) influence hydride embrittlement by affecting the hydride morphology. Besides, hydride morphology plays an important role in the delayed hydride cracking (DHC) process. DHC is mechanism for a brittle crack growth in which the crack tip acts as a sink for hydrogen in solid solution, due to diffusion in an inhomogeneous stress field, leading to the formation of a large hydride and local embrittlement near the crack tip. If the stress intensity factor (SIF) exceeds the threshold value, the hydride cracks by its length and then the process repeats. The SIF threshold and DHC kinetic is determined by the length and thickness of the hydride near the crack tip [95,96].

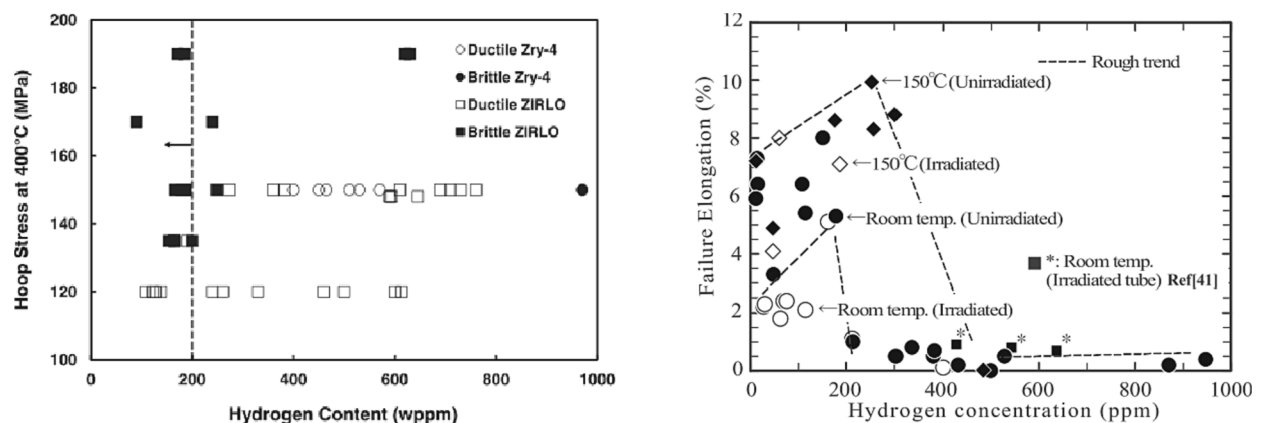


Fig. 12. Experimental evidences of nonmonotonic dependence of ductility on hydrogen content after thermomechanical cycling; (a) – data by Billone [69], (b) – data by Nakatsuka [85].

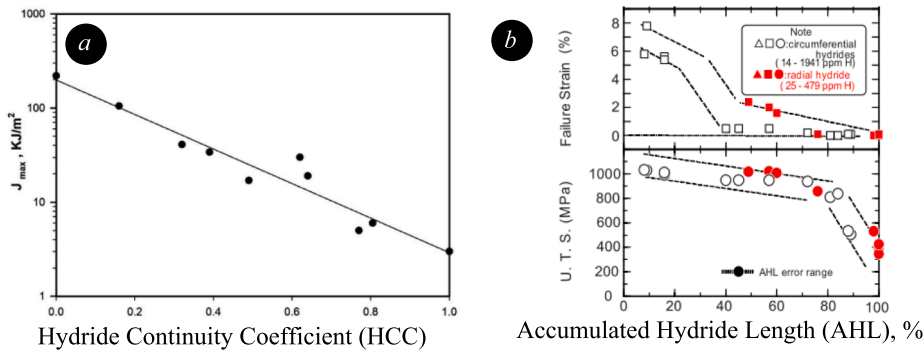


Fig. 13. Correlation between ductility and connectivity of hydrides; (a) – data by Gopalan [54], (b) – data by in Nakatsuka [85].

Conflicting data have been published on the effect of *grain size* on the hydride embrittlement degree and DBT conditions. Kim [77] assume that increasing grain size reduces hydride connectivity and, thus, raises the threshold hydrogen concentration of DBT (i.e. coarse-grained alloys have lower susceptibility to hydride embrittlement). This statement is based on the experimental data [77], according to which the threshold hydrogen concentration of DBT in Zr-2.5Nb (490 ppm at a grain size of 0.89 μm) is lower than that of Zircaloy-4 (560 ppm at a grain size of 1.86 μm). It should be noted that Kim [77] neglected other inequalities between these two alloys such as chemical composition, microstructure, texture and internal stress, which can impact the morphology of hydrides and embrittlement degree. Arsene [28] excluded influence of all factors except grain size by comparing Zircaloy-4 samples with the mean grain sizes 3 and 8 μm and got opposite conclusion to Kim [77]: increasing the grain size reduces the threshold hydrogen concentration of DBT (1200 ppm at 3 μm against 760 ppm at 8 μm , as can be seen in Table IV in [28]). Arsene [28] explain such behaviour by the fact that percolation of the intergranular hydrides' network needs lower hydrogen concentration in coarse-grained alloys than in fine-grained alloys. In coarse-grained samples, the grain boundary length per unit square of a cross-section is lower and, if hydrides occupy the grain boundary randomly, the alloy with large grains may reach the interlinked network of hydrides at lower hydrogen concentrations, creating a continuous path for brittle cracks to propagate.

The texture and metallurgical state of the alloy also affect the fracture mode due to their impact on the hydride morphology, particularly under low external stress. As it can be seen from optical micrography in Fig. 3 in Hsu [13], stress-relieved annealed (SRA) Zircaloy-4 is more prone to form prolonged hydride networks with greater connectivity in the rolling direction than the recrystallized (RXA) Zircaloy-4, which has more misoriented and discontinuous hydrides. Therefore, the ductility of RXA is superior to SRA at hydrogen concentrations below the DBT threshold, as demonstrated by Fig. 7 in [13], Figs. 5 and 7 in [28], and Figs. 5 and 6 in [76]. SEM data by Hsu [13] (Figs. 12 and 13 in [13]) confirm that secondary brittle cracks and quasi-cleavage play an important role at micro-level in macroscopically ductile fractured SRA, whereas fracture surface of RXA samples display only dimples, indicating full

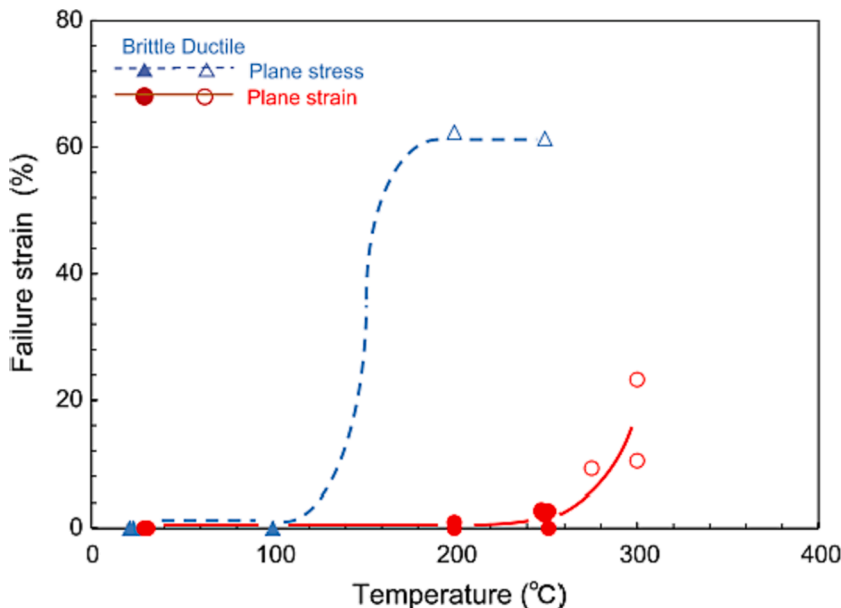


Fig. 14. DBTT shift between plane stress and plane strain in up to ~ 100 ppm radially hydrided Zircaloy-2, data by Kubo [68].

ductile fracture. Nonetheless, a prolonged hydride network that is highly connected in SRA Zircaloy-4 is strongly oriented in rolling direction and is not effective in providing a completely brittle crack path transversely, which needs for the brittle fracture of fuel rod cladding. In fuel rod cladding geometry, the SRA cladding promotes connectivity of tangential hydrides but suppresses it of radial ones. Therefore, since connectivity of radial hydrides in RXA is not suppressed as in SRA, RXA requires a lower hydrogen concentration for DBT (as shown in Figs. 5 and 7 in [28]), even despite RXA having higher ductility than SRA below the DBT threshold. This counterintuitive behavior results from loading highly-textured samples only in a pre-defined direction, simulating the real process of fuel rod cladding loading.

The *stress state* is another factor affecting the proportion of ductile and brittle fracture mechanisms. The presence of a notch in a uniaxially loaded Zircaloy-4 sample reduces the threshold hydrogen concentration of DBT at room temperature to ~ 100 ppm [29], compared to ~ 1000 ppm in an unnotched sample [28,49]. Bai [76] reported that an increase in the thickness of the tensile plate from 0.5 to 3.1 mm led to a shift in the threshold concentration from ~ 700 ppm to ~ 300 ppm. When converting from plane stress to plane strain, the DBTT in hydrogenated Zircaloy-2 significantly increases from ~ 100 °C to ~ 300 °C, as depicted in Fig. 14. Yunchang [40] provided a feasible elucidation for the stress state effect, which demonstrated that void link-up occurs at a much lower critical void density in equibiaxial tension than in uniaxial tension. Moreover, at triaxialities below 0.33, interhydride metallic ligaments exhibit increased capacity for plastic deformation; at these levels of triaxiality, the fracture mechanism for metal ligaments situated between cracked hydrides alters from voids nucleation, growth, and coalescence to one of shearing with some indication of voids formation, as described by Cockeram [14]. Another aspect of the stress state is that the *impact load* shifts the DBTT by 100 – 200 °C to higher temperatures compared to the slow load, as shown in Fig. 3 in [67].

Neutron irradiation can also increase the degree of hydride embrittlement, which should be considered when modelling of spent nuclear fuel behaviour. The majority of publications indicate that pre-irradiation increases the level of hydride embrittlement, if all other conditions being equal [85,97,98]. However, some studies report that the effect of irradiation has a level of uncertainty in measurements [87,89]. SEM-analysis of the fracture surface conducted by Nakatsuka [85] and Jang [98] indicated that the unirradiated specimen exhibit more ductile features compared to the irradiated one. The fracture surface of the irradiated samples shows a quasi-cleavage mechanism and is covered with clear brittle flat facets that are comparable to the grain size, as illustrated in Fig. 8 in [85]. According to Jang [98] (Figs. 10 and 15 in [98]), the fracture surfaces of unirradiated Zircaloy-4 samples have more secondary cracks oriented perpendicular to the fracture surface compared to irradiated ones. This difference in fracture mechanisms is likely due to shorter hydrides with higher tendency to radial orientation in irradiated samples, as displayed in Figs. 5 and 11 in [98]. Daum [82] also explains the irradiation effect in Zircaloy-4 suggesting that radially-oriented hydride formation in fuel rod cladding is more susceptible under irradiation conditions, causing stress threshold (for reorientation of hydrides) to drop from 80 MPa in unirradiated samples, to 70 MPa in irradiated ones. Auzoux [97] validates this hypothesis through their experimental data, which confirms the reduction of the reorientation threshold in Zircaloy-2; however Jang [98] reports conflicting results for Zircaloy-4. Alternatively, Tomiyasu [63] has claimed, that the primary factor for reducing the fracture toughness of high burnup fuel cladding is the formation of *hydride rim*. Kim [72] has confirmed that specimens with hydride rims can imitate the mechanical behaviour of high burnup zirconium alloys to a certain degree.

3. Theoretical approaches to the fracture problem of hydrogenated zirconium alloys

3.1. Damage nucleation

The earliest approaches to model fracture mechanics and DBT conditions in hydrogenated zirconium alloys were found on the estimating fracture stress and strain of hydrides, which were considered as parameters for the damage nucleation. Puls [38] utilized finite element method (FEM) to evaluate fracture stress by taking into account hydrides as hard precipitates embedded in a metal

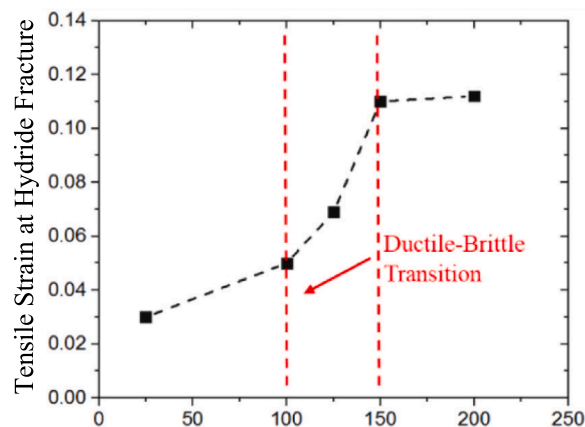


Fig. 15. Calculated tensile strain at hydride fracture on temperature; data by Wang [34].

matrix that is undergoing plastic deformation. Fracture was assumed to necessitate a crucial internal stress, which originates from the inhomogeneity of strain between the ductile matrix and the less ductile hydride. Later, Choubey [27] has applied FEM in elasto-plastic approximation and demonstrated that, according to their calculations, fracture strength of hydrides reduces with an increase of temperature from 575 MPa at room temperature to 520 MPa at 100 °C. The slight reduction in fracture strength of hydride with an increase in temperature was confirmed through experiments conducted by Shi [99] as well as later FEM calculations by Wang [34]. However, this decrease is too weak and cannot fully explain the sharp nature of DBT. Alternatively, the sample tensile strain at hydride fracture, calculated by isotropic elasto-plastic FEM by Wang [34], shows a sharp increase approximately for two times in the temperature range 100 – 150 °C, as shown in Fig. 15. This increase is due to the reduction in yield stress of hydrides with temperature, which has a stronger dependence on temperature compared to yield stress of the metal matrix. It is important to note that at room temperature, hydrides have a higher hardness than the metal matrix, but by 200 °C, this is *vice versa*, as shown in Fig. 16a here and Fig. 2b in [100]. As a result of the temperature increase, the stress in the hydride decreases, leading to a reduction in the probability of hydride fracture. Therefore, according to Wang [34], the temperature at which the yield stress in hydrides becomes lower than that of the metal defines the DBT temperature. It is worth noting, that Simpson [101] had previously proposed a similar hypothesis.

Shi [99] proposed a hypothesis that is similar to the interpretation of DBTT presented by Wang [34] and Simpson [101]. Shi [99] has determined in experiments that the fracture strength of hydride decreases with increasing temperature at a faster rate compared to yield stress of the metal, as shown in Fig. 16b. Specially, the fracture strength of hydride is lower than the yield stress of the metal below ~ 125 °C, while the opposite is true at higher temperatures, which is the root of DBT within the temperature range of 120 – 140 °C, according to Shi [99]. This hypothesis was later substantiated by experimental data obtained by Kubo [68] (Fig. 15 in [68]). According to Bind [74], the process can be explained as follows: at high temperatures, the material exhibits ductile fracture because the yield stress of the metal is lower than the fracture strength of the embedded hydride, and the matrix strength cannot generate enough stress to fracture the hydrides. Conversely, at low temperatures, the material exhibits brittle fracture because the yield stress of the metal is higher than the fracture strength of the embedded hydride, and the matrix strength can generate sufficient stress to fracture the hydrides.

The ratio of the yield stresses of the metal matrix and the hydride phase could indeed affect the crack conditions within hydrides, as demonstrated by fracture tests with various alloys. Hydrides in hardened alloys Zircaloy-2 and Zr-2.5Nb (yield stress is in the range 600 – 900 MPa) fracture at higher plastic strains ($\epsilon_c \sim 1\%$) [38], compared to hydrides in pure zirconium (yield stress ~ 300 MPa, $\epsilon_c \sim 0.2\%$) [37]. Both experiments [37] and [38] were conducted by Puls at room temperature utilizing the same acoustic emission technique.

Finally, Cherubin [102] recently suggested a third similar explanation of DBTT. They compared the hardness of hydrides and Zr-2.5Nb and found that hydrides soften more than the Zr-2.5Nb alloy at around 200 °C, which corresponds well with DBTT. Cherubin [102] assume that at low temperatures, hydrides are harder than the metal matrix and act as stress concentrators, causing brittle fracture.

All three hypotheses described above, posing that the fracture mode change resulting from an increase in temperature is the consequence of changes in the mechanical properties' ratio of metal and hydride, are supported by experiments (both directly and indirectly) and calculations. However, they do not explain the dependence of DBT on hydrogen concentration, loading scheme, and other factors.

These factors can be taken into account by considering the fracture nucleation process in more detail. A brittle crack nucleates near

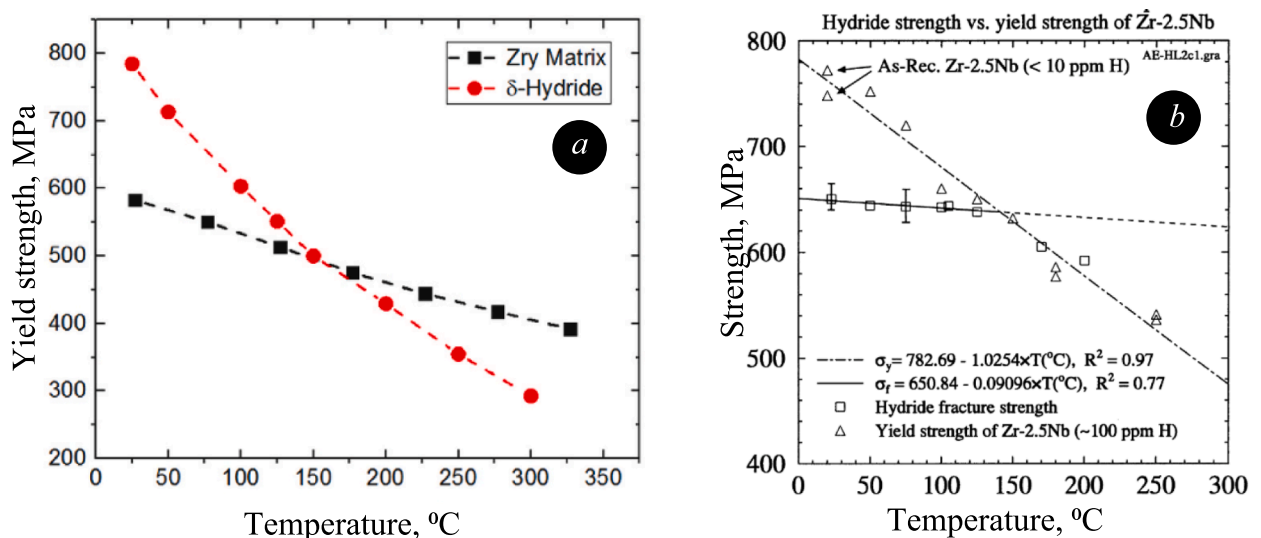


Fig. 16. Dependence of mechanical properties of hydride and zirconium on temperature, which, as assumed, can explain DBTT. Two hypothesis: (a) – DBT occurs when yield stress of in hydride becomes lower than in metal, data by Wang [34]; (b) – DBT occurs when the yield stress in metal becomes lower than the hydride fracture strength, data by Shi [99].

local stress concentrators generated by dislocation pile-ups. Therefore, the next level of detail in simulation involves considering the interaction between the metal/hydride interphase and dislocations. Ziaei [103,104] considered the possible semi-coherent orientation relationships between bcc hydrides and HCP zirconium matrix and coupled it to a dislocation density model that considered generation, interaction and annihilation for both mobile and immobile dislocations. Then, Ziaei [103,104] applied their approach to simulate the nucleation and propagation of a cleavage crack in a multigrain sample. The approach enables simulation of the stress accumulation in sample and can help to predict the brittle crack nucleation, despite some oversimplifying assumptions such as disregarding the ductile fracture mode of metal (cleavage of the metal matrix was not observed in conditions of practical interest). Besides, Ziaei [103,104] considered only intragranular hydrides, whereas intergranular ones play the main role in the fracture process. Later, Hasan [105,106,107] has developed a new machine learning framework for microstructural analysis based on this model. The framework enables the prediction of fracture nucleation in zirconium alloys with hydride populations and estimation of fracture probability. Note, that earlier, Tummala [108] also investigated the interaction of metal dislocations with hydride utilizing 3D discrete dislocation dynamics (DDD) method, albeit beyond the scope of fracture problems.

The most detailed and basic approach for simulating the brittle crack nucleation is to consider the stress concentrator itself. Ghaffarian [109] investigated the process of dislocations passing through the metal/hydride interphase under uniaxial load of a polycrystalline sample, using the molecular dynamics (MD) simulation method. The study revealed that the number of stress concentrators on the surface of the hydrides depends on their size, orientation, and intersection length with the dislocation line. Reali [44,110,111] implemented the discrete dislocation plasticity (DDP) approach for the same aim. Their findings highlighted the significant influence of the interface's permeability, alongside the presence of dislocation sources within the hydride and intersections between edge and screw dislocations, plastic stress relaxation [110], misfit stress and dislocation structure surrounding the hydride [110,111]. Their approach simulates principal and shear stresses near the concentrator, dislocation and energy densities at pile-ups where a slip band intersects the Zr/hydride interface. Fig. 17 illustrates some findings of Reali [111]. The approach currently under development by Reali and co-authors is crucial for comprehending the damage nucleation process, and needs to be expanded to intergranular hydrides as well.

3.2. Growth and coalescence of cracks

According to the phenomenological model developed by Arsene [28], the DBT in hydrogenated zirconium alloys is predominantly caused by crack propagation instead of their nucleation. This approximation predicts that fully brittle fracture is only possible if the initial crack (a cracked hydride) is able to induce brittle fracture of the neighboring hydride. If applicable, the DBT is determined by two parameters: hydride length and distance between hydrides. The distance between hydrides must be small enough for brittle fracture, as well as the fracture toughness of the metal ligament. Arsene [28] stated that the critical distance between hydrides, allowing for crack propagation, is $0.5 \mu\text{m}$, although this value may depend on temperature and loading scheme. Tseng [112] investigated the impact of hydrides in the vicinity of the crack tip on crack propagation, applying a 2D elastic FEM-model and found that the morphology of the hydrides was a strong factor. However, the elastic approach ignores the plastic zones near the crack tips in metal ligaments which plays an important role in crack propagations, [28]. Moreover, the plastic zone adjacent to the crack tip provides shielding of the stress field, thereby preventing the brittle fracture of neighboring hydrides. This phenomenon is supported by the features of DHC process, which is not observed above temperatures of $\sim 350 \text{ }^\circ\text{C}$, *i.e.*, brittle fracture of a hydride near the crack tip does not occur at high temperatures, as shown in Figs. 8 and 9 in Resta Levi [113]. Analytical models developed by Shi [95] and Aliev [96] explain this behavior due to temperature dependence of the metal yield stress, as displayed in Fig. 18 here and Fig. 10. 22 in [2]. According to the interpretation of Aliev [96], the plastic zone present near the crack tip shields the stress field at high temperatures and protects hydrides from the brittle fracture. The crack blunting is an additional important factor that may prevent brittle crack growth, thereby limiting DBTT from above.

Another significant area of theoretical research into the fracture mechanisms for hydrogenated zirconium alloys is focused on examining the fracture of the matrix ligament between hydrides, which leads to the coalescence of cracks and plastic flow localization. Chan [114] considered hydrides in zirconium-based alloy as a lattice of equivalent microcracks. In this assumption, the fracture of the

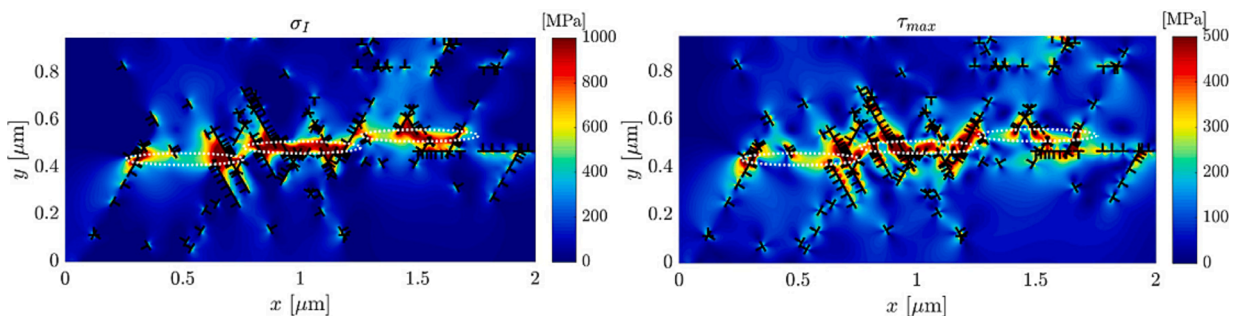


Fig. 17. Maximum principal σ_I (left) and shear τ_{max} (right) stress at pile-ups where slip band intersects the Zr/hydride interphase boundary. Calculations and plot from Reali [111].

sample occurs due to the collapse of ligaments between cracked hydrides. Mathematically, this condition represents the threshold plastic strain in the metal ligament required for its fracture. Chan [114] estimated this threshold analytically in 2D approximation by considering the interaction of two neighbouring cracks. The resultant mechanical field in the ligament depends on the length of the cracks and distance between them, enabling an interlinking of hydride morphology and fracture conditions. The morphology of hydrides is modelled with a single parameter “continuity of hydride network”, which is determined by the relationship between the volume fraction of hydrides, their length and the distance between them. The model of Chan [114] describes the observed impact of the volume fraction of hydrides on normalized ductility, including a sharp reduction in ductility resulting from the formation of an interconnected hydride network. Based on the analytical approach of Chan [114], Nilsson [115] developed a 2D FEM-model to simulate the elasto-plastic mechanical behaviour of the ligament between cracked hydrides. To estimate J -integral, Nilsson [115] considered a real morphology of hydrides rather than a regular lattice, as it assumed by Chan [114]. Nilsson [115] conducted FEM calculations that establish that the fracture toughness of a specimen relies on the configuration of a local hydride cluster, and the key morphology parameters are orientation of hydrides to external stress, their length and distance between hydrides. Another extension to the approach of Chan [114] is represented by the analytical model of Qin [116]. In contrast to Chan [114] and Nilsson [115], Qin [116] rejects the idea that all hydrides crack simultaneously at the initial stage of plastic deformation. Instead, they proposed that the longest and/or intergranular hydrides are the first to crack. This results in including uncracked hydrides in the ligament between the cracked ones, which reduces the critical plastic strain in the ligament. Nevertheless, the ligament fracture condition mathematically aligns with models of Chan [114] and Nilsson [115]: the ligament fractures when the local strain reaches a critical level. Another feature of the Qin’s [116] approach is that they accounted for the hydrides’ growth in the specimen with a permanent hydrogen source (due to oxidation, for example). In this approximation, they estimated time until DBT at typical operational conditions of the fuel rod cladding.

Liu [117] had developed a 3D FEM model that challenges the basic assumption of Chan [114] that hydrides are already fractured. Instead, Liu [117] proposed that damage nucleation occurs due to the separation of the hydride/matrix interface along the hydride. However, this contradicts experimental data. Another weakness of the model lies in its parameter determination through calibration with experimental data that exhibit significant statistical scatter (40 – 100 % of the relative value, according to Fig. 6 in [117]). Nevertheless, despite the weak verification, the model of Liu [117] demonstrated the potential to the mechanical behavior of macroscopical samples under various loading scheme (dog-bone notched and smooth samples, fuel rod cladding and others). An important feature of the approach developed by Liu [117] is the ability to predict the maximum equivalent plastic strain in the ligament as a function of the stress triaxiality.

3.3. Percolation of a brittle crack (hydride morphology modelling)

The morphology of hydrides has a significant impact on fracture mechanisms, and the formation of an interconnected hydride network can lead to DBT. This is supported by experimental data and theoretical models from Chan [114], Nilsson [115], and Qin [116], who have considered the hydride morphology as an external parameter in their modelling. In this context, the DBT problem can be reduced to the task of brittle crack percolation and modeling the hydride morphology.

Arsene [28] assumed that an interlinked network of hydrides forms when hydrides fully occupy grain boundaries in the metal. Based on this assumption, they obtained a qualitative agreement with experimental data demonstrating that finer grain size require higher hydrogen concentration need for DBT. However, Arsene’s approach [28] overestimates the threshold hydrogen concentration. This is because a hydride network with the required connectivity for DBT forms when there is only partial occupation of grain boundaries, not a total one, as assumed for simplicity by Arsene [28]. Qin [118] also considered the problem of interlinked hydride network formation; however, their approximation does not involve random hydride nucleation. They assumed that a new hydride typically nucleates close to the tip of an already existing one within the nearest metal grain or at the grain boundary, depending on the

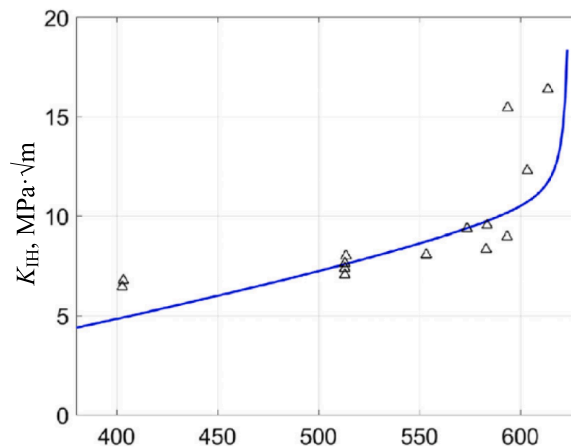


Fig. 18. Dependence of the threshold stress intensity factor (K_{IH}) of DHC on temperature, calculations by Aliev [96]; markers – experimental data by Resta Levi [113].

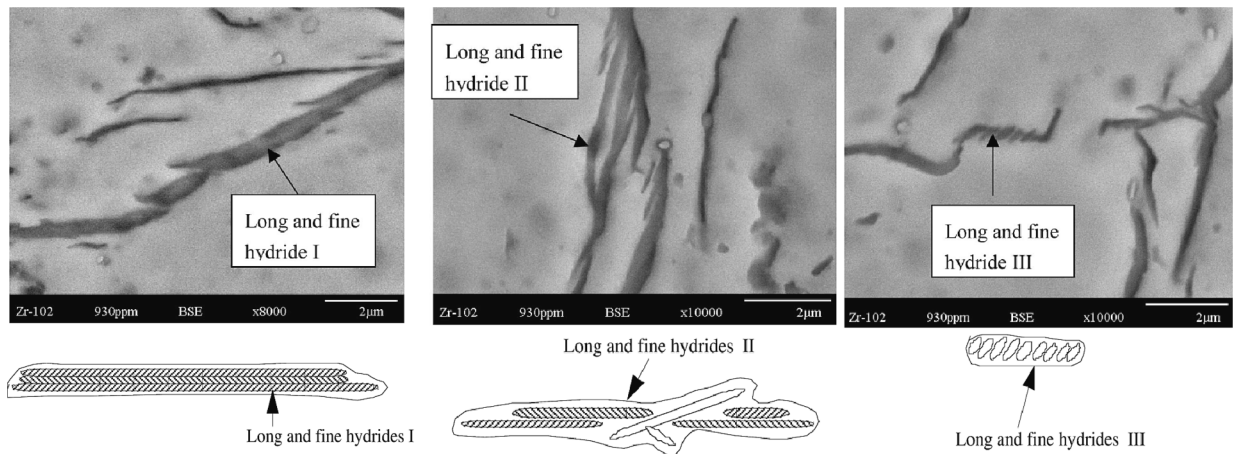


Fig. 19. Different stacking orders of nanoscale hydrides. SEM data by Veleva [120].

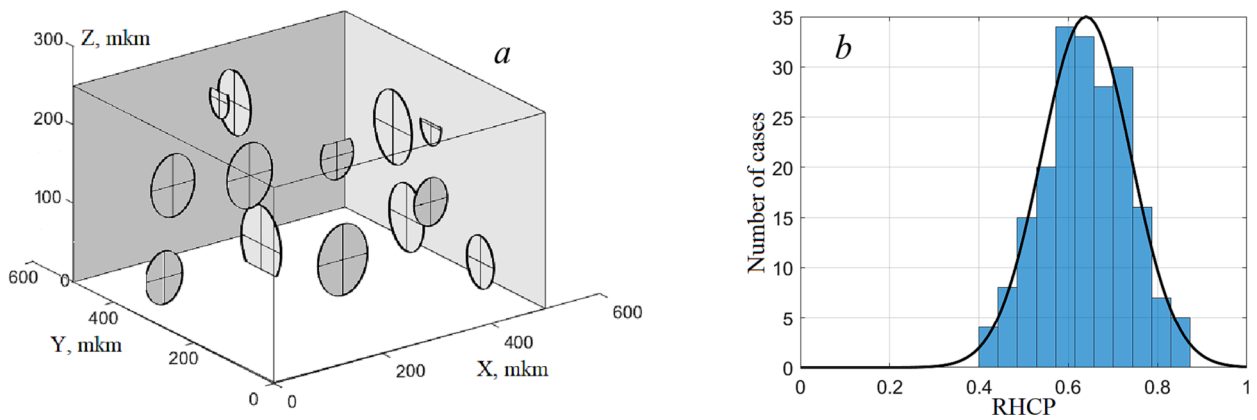


Fig. 20. Numerical simulation of hydrides in 3D domain by Aliev [141]; a – 3D domain and hydrides as discs with two possible orientations; b – calculated distribution of a morphology metric RHCP, determined in [94].

local stresses and the grain boundary energy. As a result, Qin [118] were able to ascertain the correlation between threshold hydrogen concentration for DBT and the metal's texture (including the misorientation and size of metal grains). The study by Qin [118] demonstrates excellent consistency with experiments: at temperatures 673 and 721 K the calculated threshold hydrogen concentration for the formation of continuous hydride network within the sample (and, consequently, DBT) was estimated as 590 and 820 ppm, while the experimental values were 600 and 850 ppm, respectively.

The texture and microstructure of the alloy solely determine hydride morphology under sufficiently low external stresses. However, external stress that exceeds the threshold value (~ 100 MPa) becomes the main determinant of hydride orientation, as hydrides tend to orient perpendicular to the external tension. The mechanism of reorientation remains unclear and lacks a common explanation. The complexity of this problem arises from the fact that microscale hydrides have a complicated structure of nanoscale hydrides (both inter- and intragranular ones) forming a two-dimensional surface, also known as a stack, for example EBSD data on Fig. 4 in [119] and synchrotron X-ray tomography data in [3]. Several hypothesizes have been proposed to elucidate the mechanism of hydride reorientation under external stress: (1) varied stacking order of nanoscale hydrides, (2) change of the habit plane, and (3) different nucleation sites activation.

A reorientation mechanism, frequently discussed in literature, involves the varied stacking order of nano hydrides, whose orientation relationships are not reliant on external stress. The experimental observation and graphical interpretation are presented by Veleva [120] and shown in Fig. 19. This mechanism was verified through phase-field calculations by Han [121] and Heo [122]. However, another phase-field simulation carried out by Simon [123] did not confirm the hydride reorientation caused by the different stacking of nanoscale hydrides due to external stresses. This discrepancy has not been commented by the authors of the calculations. Unfortunately, phase-field models have not yet accounted for the influence of hydrides on the mechanical properties of zirconium alloys, despite the potential to do so. For instance, Kharchenko [124] utilized the phase field method to simulate both the morphology of β -phase in Zr-1 %Nb-1 %Sn alloy and the interaction of these inclusions with dislocations in the metal matrix during plastic deformation.

Both the habit plane selection of hydrides and their nucleation sites are influenced by applied external stress, as per EBSD findings presented by Kiran Kumar [125]. In stress-free samples both intergranular and intragranular hydrides are found to conform with the $(0001)_{\alpha\text{-Zr}}// (111)_{\delta\text{-ZrH}}$ orientation relationship, and preferred nucleation sites are located at grain boundaries, which are almost parallel to the basal plane in one of the neighboring grain. In contrast, the hydrides formed in the presence of external tension mainly follow the $(10\text{--}11)_{\alpha\text{-Zr}}// (111)_{\delta\text{-ZrH}}$ relationship, but relationships $(10\text{--}17)_{\alpha\text{-Zr}}// (111)_{\delta\text{-ZrH}}$, $(10\text{--}13)_{\alpha\text{-Zr}}// (111)_{\delta\text{-ZrH}}$ and $(10\text{--}10)_{\alpha\text{-Zr}}// (111)_{\delta\text{-ZrH}}$ are also occasionally observed. Moreover, hydrides tend to form at grain boundaries aligned perpendicularly to external tension [125], indicating a shift in preferential nucleation sites. Toghraee [126] have reported that phase field calculations estimate the magnitude of applied strain required to change a single hydride's habit plane to be ~ 0.02 , which is one order higher than the experimental value. Nevertheless, the presence of neighboring hydrides may markedly decrease the stress needed for reorientation, making it comparable to the experimental results [126].

An analytical model developed by Qin [127] allows estimating the stress threshold for hydride reorientation caused by changes in orientation relationships and preferred nucleation sites on grain boundaries in the presence of external stress. The model is based on evaluating the Gibbs energy for inter- and intragranular hydrides with various nucleation sites and orientation relationships. Thereby, Qin [127] simulate the dependence of the lower threshold (the stress level at which reorientation begins) and higher threshold (the stress level at which full reorientation occurs) on the mechanical properties of the metal matrix, temperature and texture.

An alternative method for simulating the morphology of hydrides in zirconium alloys relies on semi-correlation relationship between the orientation of hydrides and external stress, and is typically applied for practical purposes. The first model within this framework was formulated by Ells [128]. A fundamental assumption was made, which is that the orientation of hydrides is determined by the that of its nucleus, thereby determining the type of the correlation. The model parameters in this correlation are calibrated against experimental data. Later, Hardie [129] and Bai [130] employed a similar method in their experiments to simulate the fraction of reoriented hydrides under external stress. Puls [131] modified this approach by taking into account internal stresses. The model of Ells [128] is also a basis for a number of computational tools which predicts the orientation of hydrides in zirconium fuel rod cladding during operation and post-operational storage of nuclear fuel, [132,133,134,135,136]. Feria [137] introduced a semi-correlational alternative model that rests upon an assumption of linear dependence between the fraction of reoriented hydrides and external stress.

The degree of hydride embrittlement is determined not solely by the orientation of hydrides, but also by other hydride morphology parameters like their length, volume density and connectivity. To determine all the morphology parameters, the approaches developed by Chan [138] and Kolesnik [139] take into account hydride nucleation in a classical heterogeneous approximation. The next generation of models by Kolesnik [140] and Aliev [141] simulates detailed morphology of hydrides in a 3D domain, as shown in Fig. 20a. Nucleation is assumed to occur on predetermined sites within the metal matrix, such as triple points, grain and phase boundaries, and intersections of dislocations. Distribution functions of nucleation sites by space and energy is defined by user before the calculation as external parameters of the model. The growth of hydrides is simulated upon through an analytical solution of the diffusion task that considers misfit stress and competition amongst adjacent hydrides for hydrogen in solid solution (in simplified approach according to [141]). The model simulates both the mean value and distribution width of any morphology metric, such as length, orientation, and connectivity, for example, the calculated radial hydride continuous path (RHCP) in Fig. 20b.

3.4. Fracture strain modelling (continual approach)

An alternative viewpoint on the modeling of hydride embrittlement involves analyzing zirconium alloys with hydrides using a continual approach. The ground model in this approach is based on the theory of spherical void growth in a yielded matrix, introduced by Rice and Tracey [142]. According to their model, the plastic strain resulting in fracture (when the voids' coalescence occurs) can be predicted given the initial porosity and load triaxiality. Arsene [28] applied the model of Rice and Tracey [142] to simulate the behaviour of hydrided zirconium alloys. However, they were unable to describe a function of fracture plastic strain on the hydrogen content and, therefore, DBT at room temperature. This may be attributed to the fact, that at room temperature brittle cracks of hydrides exhibit minimal opening and are non-spherical, thereby contradicting to fundamental assumptions of Rice and Tracey's theory [142]. In contrast, at 300 °C initial brittle cracks of hydrides open up as nearly spherical shapes in plastic matrix and the model developed by Rice and Tracey [142] effectively describes well this type of fracture, as stated by Arsene [28].

The theory of Rice and Tracey [142] can also be applied to fracture modelling of non-hydrided zirconium alloys, as demonstrated Cockeram [17]. They modified the original model by considering the distribution of initial void radii to take into account various damage nucleation sites: (a) slipband decohesion, (b) intersecting slipbands, (c) impinging slip on grain or lath boundaries and (d) grain boundary or lath boundary intermetallic particles. The model of Cockeram [17] describes experimental dependence of effective strain on load triaxiality. In another publication, Cockeram [143] analysed non-hydrogenated Zircaloy-4 and explored unstable crack extension, thereby identifying three potential crack growth mechanisms based on experimental observations: (a) tearing along slip bands, (b) the nucleation, growth, and coalescence of voids with the crack tip, and (c) a combination of tearing along slip bands with and without void nucleation, growth, and coalescence. Furthermore, they developed an analytical model for the second fracture mechanism based on the continual theory. The model postulates that void nucleation occurs on Laves phases $\text{Zr}(\text{Cr},\text{Fe})_2$ in three steps if plastic strain surpasses the critical value: (a) slip impingement at a particle, (b) particle cracking, and (c) particles' interface decohesion. The simulation of voids' growth and coalescence is based on the theory of Rice and Tracey [142], but by taking into account the fact that voids near the crack tip are in an inhomogeneous field of mechanical stress simulated in the approximation of Hutchinson-Rice-Rosengren (HRR), based on Hutchinson [144] and Rice and Rosengren [145]. According to HRR asymptotic solution, power-hardening material stresses within the plastic zone remain independent of the distance to the tip and depend only on the angle formed by the crack plane and by the direction to the tip. The model developed by Cockeram [143] estimates the critical stress

intensity factor (SIF) required for plastic crack growth. While Cockeram and Chan did not take into account the impact of hydrides on the fracture process, it remains applicable in predicting the growth of ductile cracks in the ligament between hydrides.

Further development of the continuum damage mechanics is associated with the Gurson's model [146]. Gurson defined the yield criterion and the flow rule for porous material as functions on stress-state triaxiality for rigid-plastic approximation. Plastic strain growth causes the volume fraction of voids to rise, and eventually leads to sample fracture when the porosity reaches the critical level. Later, Needleman and Tvergaard [147] modified the Gurson's model by taking into account interaction between pores, their coalescence and nucleation of new ones, and, thus, the modified approach is known as Gurson-Tvergaard-Needleman, or GTN-model. This model has been successfully utilized for simulating mechanical behaviour in unhydrogenated zirconium alloys, such as Zr-2.5Nb by Williams [148] and β -treated Zircaloy-4 by Zhou [149].

Prat [150] applied GTN-model to simulate the fracture of hydrogenated zirconium alloys. They considered two mechanisms of void nucleation: brittle fracture of hydrides and void nucleation in the metal matrix. For both mechanisms, the damage evolution was assumed to be linear on plastic strain above the threshold values (hydride fracture occurs after necking). Prat [150] demonstrated a good agreement with experiments for calculated dependence of fracture strain on hydrogen content for both smooth and notched samples at room temperature. However, the model slightly overestimates the plasticity of notched samples in the 400 – 1000 ppm range, potentially due to the simulation of void nucleation at fractured hydrides, ignoring the influence of stress and triaxiality. Later, Grange [151] extended GTN-model by accounting for plastic anisotropy and viscoplasticity and applied this model to simulate the ductile fracture of hydrided Zircaloy-4. Le Saux [152] adjusted the parameters of the model developed by Grange [151] and used their own new experimental data [12] to validate the model under wide-ranging temperatures and loading schemes. Le Saux [152] also assumed that damage nucleation occurs both on fractured hydrides and Laves phases, with the latter being more prevalent in unhydrided samples and at elevated temperatures.

The GTN-model effectively describes the growth of ductile crack and ductile fracture in the sample by taking into account nucleation, growth and coalescence of voids. However, the GTN-model necessitates the definition of several model parameters, some of which are non-physical, such as coefficients of correlations. This fact significantly restricts the practical usage of the GTN approach.

An alternative to GTN approach is to apply the cohesive zone model (CZM), also known as Dugdale model, based on the pioneering works of Dugdale [153] and Barenblatt [154]. CZM considers the narrow region near the crack tip as a cohesive traction between the bounding surfaces. Hillerborg [155] and Needleman [156] modified the CZM concept by coupling it with the FEM, defining a cohesive zone element that follows the traction-separation law. Cohesive traction T_n is determined as a function of the separation δ_n as $T_n = \sigma_{\max} f(\delta_n)$ (σ_{\max} is the peak value of traction and the function $f(\delta_n)$ defines the traction-separation law), and the area under the plot is the cohesive energy. Cornec [157] demonstrated that both parameters (cohesive traction and cohesive energy) can be determined by experiments. This results in a significant advantage for the CZM approach when compared to the GTN-model and makes CZM more suitable for practical application. Note, that Wäßling [158], Kim [159] and Matvienko [160] applied CZM-based models to simulate the threshold value of stress intensity factor (SIF) in the DHC problem in zirconium alloys, however this is beyond the scope of this research.

Subsequently, Banerjee [161] developed the traction-separation law which takes into account the stress-state triaxiality using only two model parameters, but gives the same simulation results as the GTN model using more model parameters. Recently, Fang [162] applied the CZM approach in the interpretation of Banerjee [161] to simulate the mechanical behavior of hydrogenated zirconium alloys. They described the dependence of the crack tip opening displacement (CTOD) on external tension. Fang [162] simulated the impact of hydrides by incorporating an element with specific mechanical properties into the cohesive zone, to model hydrides. This facilitated an examination of the impact of hydride size and morphology on the force/CTOD diagram. Fang [162] cross-verified their results using FEM-based code developed by Chen [163]. In their subsequent paper, Fang [164] conducted 2D simulations and demonstrated that the fracture behavior of a hydrogenated zirconium sample is dependent on the cohesive strength of the zirconium alloy, alongside the number density and arrangement of hydrides.

A continual approach developed by Chen [165] is different from all models described above. The mechanical behaviour of the hydrogenated Zircaloy-4 in [165] is derived using a stored potential strain-energy function. The model is FEM-based and uses 3D approximation for isotropic elastoplastic material. The hydrides are represented as elastic brittle inclusions. The mechanical energy density function relies on the volume fraction of hydrides that have two perpendicular orientations, which are external parameters of the model. The model of Chen [165] simulates the diagram of large deformations and load vs. displacement of ring compression tests, however the model lacks fracture prediction capabilities.

3.5. Alternative approaches

Kulkarni [166] utilized the crystal plasticity finite element method (CPFEM) to forecast the effect of hydride volume fraction, their orientation, and distance between hydrides on the mechanical properties of a zirconium alloy. The simulations were conducted using a 3D representation, featuring hundreds of metal grains within the representative volume. A notable simplification of the model is the neglect of the alloy texture; grains are assumed to be equiaxed with a random orientation. Another simplification is to solely consider intragrain hydrides, whereas intergrain hydrides can be prevalent or a vital component, as demonstrated, for example, by El Chamaa [167] and Kiran Kumar [125]. Furthermore, intergrain hydrides are known to play a dominant role in the fracture process, according to Silva [49]. The fracture condition of hydride was defined by Kulkarni [166] as the point at which the local accumulated plastic strain exceeds a critical value, which is dependent on the stress triaxiality through the correlation. The fracture threshold correlation takes the same form as the one in Liu [117] (the model by Liu [117] was discussed above), however Kulkarni [166] understand it as a condition of brittle fracture of hydrides, while Liu [117] as a condition for ductile fracture of the metal in the ligament between

hydrides. The accumulated plastic strain at hydride fracture, calculated by Kulkarni [166], is approximately 0.03, which is in close agreement with the experimental value reported by Huang [29]. Additionally, the approach by Kulkarni [166] predicts a comparable hydrogen hardening degree (*i.e.* a growth in yield stress with increasing hydrogen concentration) to that observed in the experimental data.

Finally, Singh [100] put forward an original hypothesis that suggest the fracture mode changes in hydrogenated zirconium alloys due to the thermal treatment history of the sample. According to Singh [100], the growing hydride undergoes compression because of the volume dilatation in phase transition, whilst the metal matrix near the hydride tip experiences tension. This condition is commonly observed in hydrides at room temperature following cooling. If a sample with hydrides is heated and the hydrides partially dissolve, their stress state changes to the opposite. The metal matrix close to the hydride tip compresses, thus increasing the crack resistance of hydrides after heating. FEM calculations by Singh [100] based on a linear elastic and perfectly plastic solids approach for both matrix and hydrides, demonstrated that the effect becomes significant at 150 °C, which is close the DBT temperature in certain experiments. To validate their hypothesis and determine the impact of the approach direction on the test temperature (through cooling or by heating), Singh [168] conducted an empirical investigation on Zr-2.5Nb alloy. Their analysis revealed that the approach direction did not significantly impact the fracture toughness below and above the DBT temperature; however, there was a discernible effect in the transition regime, as indicated in Fig. 21. At micro-level, the experiments revealed that the fracture surface exhibited greater axial splitting after heating compared to the surface after cooling. These disparities can be explained by the impact of dilatational stresses induced by the phase transition. Therefore, the hypothesis has an experimental confirmation, however the effect appears not to be forceful enough to determine the DBT temperature.

4. Discussion

Hydrogen significantly impacts the mechanical properties of zirconium alloys in various ways. When hydrogen is in solid solution, it decreases the mechanical strength, whereas the hydride phase has the opposite effect and increases it. Additionally, severe hydride embrittlement mechanisms have been observed. At low concentrations in hydride phases or at high temperatures (when hydrides lose their brittleness), the embrittlement of Zircaloy-4 appears to be caused by an increase in Laves phase volume due to hydrogen adsorption and the interaction between Laves phase and hydrides nucleated on its surface. However, the primary impact of hydrogen on the mechanical properties of zirconium alloys is the embrittlement resulting from the presence of the brittle hydride phase.

There are three embrittlement mechanisms that can be associated with the hydride phase in zirconium alloys (by analogy with Chan [114]): (1) a reduction in the threshold plastic strain required for microcrack nucleation due to the fracture of brittle hydrides, (2) the provision of easy pathways for brittle crack propagation through the continuous network of hydrides, and (3) an increase in the plastic flow concentration in the metal ligaments between hydrides due to a decrease in the effective plastic cross-section. Thus, the DBT problem in hydrogenated zirconium alloys can be broken down into three sub-tasks (corresponding to the mechanisms mentioned above): (1) on the damage nucleation; (2) on the brittle crack percolation, and (3) on the growth and coalescence of cracks and/or voids. Each mechanism determines different parameters of DBT (temperature, continuity of hydrides' network, plastic strain, triaxiality) on various degree. The selection of a particular task depends on the parameter of DBT that is of greatest interest. Further details on these tasks and related parameters are discussed below.

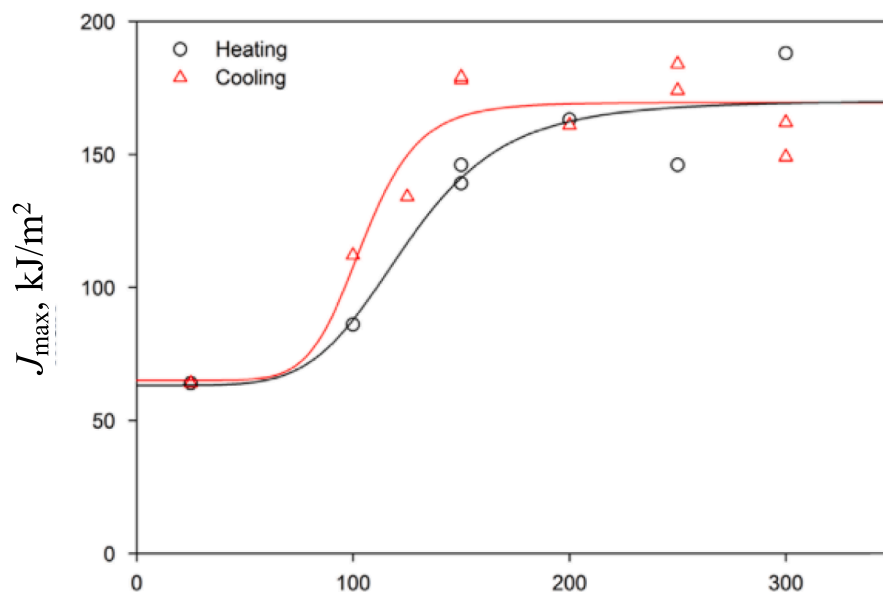


Fig. 21. The effect of direction of temperature approach on fracture toughness and DBT. Cooling – higher line, heating – lower line; data by Singh [168].

Task 1. On the damage nucleation (fracture of hydrides).

Brittle fracture of hydrides (if it occurs) is the dominant mechanism for damage nucleation in hydrogenated zirconium alloys. However, hydride brittleness is sensitive to temperature and is not observed at high temperatures. Therefore, the task on damage nucleation allows determining the temperature of DBT. The influence of triaxiality and local plastic strain in the slip band on DBT temperature can also be considered in the scope of this task. Most likely, the ductile to brittle transition resulting from an increase in temperature is associated foremost with the change in the mechanical interaction between the hydride and the ambient metal matrix, rather than other factors. The partial dissolution of hydrides upon heating cannot sufficiently account for this phenomenon. On the contrary, minimal volume fraction of the hydride phase causing brittle fracture mode increase with the temperature. According to experimental data by Arsene [28], the DBT threshold hydrogen concentration at 20 and 300 °C are 800 and 2200 ppm, respectively (solubility at 300 °C is below 100 ppm, according to Zanellato [169] and can be neglected in comparison with 2200 ppm). The effect of local dilatation stresses due to partial dissolution of hydrides is weak and also cannot explain the DBT, as shown in Fig. 21 in [168]. Apparently, hydrides lose their brittleness at high temperatures (above DBT temperature, or DBTT) because the yield stress of the metal matrix becomes lower than the yield stress [34,101] and/or fracture strength [68,99] of embedded hydrides, and therefore, the weak metal matrix is not able to generate sufficient stress to fracture hydrides [74]. While at lower temperatures (below DBTT), the yield stress of the metal matrix, on the contrary, is higher than the fracture strength of hydrides, and internal stresses in metals can cause a brittle crack [74]. This hypothesis is supported by both experimental and calculated evidences. However, current theoretical approaches are still unable to simulate the DBTT dependence on stress triaxiality. Potentially, the strong temperature dependence of the ductility near the DBTT can be described by the exponential function of void nucleation. If one elucidates the void nucleation process at a micro-level, taking into account the interaction between brittle hydride and pile-up of metal dislocations in the slip band, the task can be accomplished.

Task 2. On the brittle crack percolation (morphology of hydrides).

The second mechanism of hydride embrittlement of zirconium alloys is providing the easy pathway for the brittle crack propagation through the continuous network of hydrides. This is due to the formation of a hydride cluster with critical parameters, resulting in DBT and allowing for a continuous pathway through the sample (*i.e.*, the brittle crack percolation). The percolation phenomenon can explain the threshold nature of ductility dependence on the hydrogen content, as displayed in Fig. 10. Thus, the relevant parameter of DBT in the scope of this task is the continuity of hydride network and it ultimately reduces to the simulation of hydride's morphology. This task can be sub-divided into two sub-tasks: (1) finding the threshold hydrogen concentration and (2) identifying the optimal thermomechanical loading scenario to prevent the formation of an interconnected network of hydrides. The first subtask represents a classical percolation problem, where hydrides randomly occupy grain boundaries. The second sub-task holds significant practical importance for the safety justification of spent nuclear fuel storage and handling regimes. This is particularly relevant when the hydrogen concentration in the zirconium fuel rod cladding remains constant, and the thermomechanical load should be limited to avoid the formation of a critical hydride morphology. Numerous models have been developed to address this task, however the majority of them only predict radial hydride fraction in fuel rod cladding and are validated in a relatively narrow range of conditions. A new approach [141] has been recently published, which predicts various continuity metrics of hydride network.

Task 3. On the growth and coalescence of cracks and/or voids (fracture of the ligament).

The presence of hydrides in zirconium alloys can increase the plastic flow concentration in metal ligaments between hydrides. The primarily objective of this task is to forecast the fracture plastic strain. Typically, this approach takes into account plastic deformation and ductile fracture regimes, while the DBT being a boundary case. In the context of hydrogenated zirconium alloys, the task is pertinent to the conditions of reactivity-initiated accident (RIA) or impact loading (for instance, during transport operation with spent nuclear fuel), wherein intense short-time mechanical loading takes place. For the task solution, continual theory methods (GTN model and CZM), crack and voids growth and coalescence approaches, and models based on Chan approach [114] have been successfully applied. This task allows developing an integral approach for simulation of fracture in hydrogenated zirconium alloys. However, the input data for such a model (hydride morphology and the critical plastic strain of hydride fracture) are solutions obtained from the prior two tasks.

5. The list of experiments

Experimental studies on the hydride embrittlement of zirconium alloys have been compiled into an open online list of experiments accessible through the following link: <https://docs.google.com/spreadsheets/d/1CKc31AljrUiOav0bEmu47CnnwEaTpPxQExf7tp2S9r4/edit#gid=0>. The list comprises over one hundred experiments, providing references, main parameters of experiments and a list of measured parameters. The list of experiments will be continuously updated as new experiments are published.

6. Conclusion

The hydride embrittlement of zirconium alloys is almost always associated with the presence of a brittle hydride phase. In conditions typical for the lifecycle of nuclear fuel (operation, transportation and post-operational storage), the brittle fracture nucleates and is localized in the hydride phase, while metallic ligaments between hydrides fracture in a ductile mode. The macroscopic fracture mode changes from ductile to brittle, if the following conditions are simultaneously satisfied:

1. hydrides must be capable of brittle fracture to serve as sites for brittle crack nucleation,
2. the nucleated brittle crack must be capable of growth to induce the brittle fracture of the subsequent hydride near the crack tip,

3. hydrides must form an interconnected network that could provide an easy pathway for the propagation of the brittle crack.

Zirconium hydrides lose their brittleness when they are heated. This fact can explain the change of the macroscopic fracture mode from brittle to ductile at elevated temperatures. This change has been confirmed by both experimental data and calculations, indicating that the fracture mode change can be attributed to the temperature dependency of the mechanical properties of the alloy and the hydrides. However, the existing models do not account for the initiation of fracture at the intersection of the slip band and hydride surface, and therefore fail to simulate the dependence of DBT temperature on the stress triaxiality. Additionally, elevated temperature can impede crack propagation by shielding the mechanical stress field near the crack tip with the plastic zone of the metal. The temperature limit for the brittle crack propagation is usually higher than that for the brittle fracture of hydrides.

The problem of interlinked hydride network formation can be classified as a classical brittle crack percolation problem. The ultimate objective of hydride morphology modeling is to forecast morphology parameters that characterize the connectivity of the hydride network in radial direction.

The complete DBT model requires a self-consistent solution of damage nucleation, brittle crack growth and percolation problems.

Funding

This research was supported by the Scholar Rescue Fund of the Institute of International Education (IIE-SRF).

Declaration of competing interest

The authors declare that they have no known competing financial interests or personal relationships that could have appeared to influence the work reported in this paper.

Data availability

No data was used for the research described in the article.

References

- [1] M.B. Djukic, G.M. Bakic, V.S. Zeravcic, A. Sedmak, B. Rajicic, Hydrogen embrittlement of industrial components: Prediction, prevention, and models, *Corrosion* 72 (7) (2016) 943–961, <https://doi.org/10.5006/1958>.
- [2] M.P. Puls, *The effect of hydrogen and hydrides on the integrity of zirconium alloy components*, Springer-Verlag, London, 2012.
- [3] Q. Fang, M.R. Daymond, A. King, Study on the morphology of bulk hydrides by synchrotron X-ray tomography, *Mater. Charact.* 134 (May) (2017) 362–369, <https://doi.org/10.1016/j.matchar.2017.11.013>.
- [4] D.O. Northwood, U. Kosasih, Hydrides and delayed hydrogen crack in zirconium and its alloys, *Int. Met. Rev.* 28 (2) (1983) 92–121, <https://doi.org/10.1179/imtr.1983.28.1.92>.
- [5] B. Cox, Environmentally-induced cracking of zirconium alloys - A review, *J. Nucl. Mater.* 170 (1) (1990) 1–23, [https://doi.org/10.1016/0022-3115\(90\)90321-D](https://doi.org/10.1016/0022-3115(90)90321-D).
- [6] J. Bair, M.A. Zaeem, M. Tonks, A review on hydride precipitation in zirconium alloys, *J. Nucl. Mater.* 466 (2015) 12–20, <https://doi.org/10.1016/j.jnucmat.2015.07.014>.
- [7] S. Suman, M.K. Khan, M. Pathak, R.N. Singh, J.K. Chakravarty, Hydrogen in Zircaloy: Mechanism and its impacts, *Int. J. Hydrogen Energy* 40 (17) (2015) 5976–5994, <https://doi.org/10.1016/j.ijhydene.2015.03.049>.
- [8] E. Conforto, I. Guillot, and X. Feaugas, "Solute hydrogen and hydride phase implications on the plasticity of zirconium and titanium alloys: A review and some recent advances," *Philos. Trans. R. Soc. A Math. Phys. Eng. Sci.*, vol. 375, no. 2098, 2017, doi: 10.1098/rsta.2016.0417.
- [9] A.T. Motta, et al., Hydrogen in zirconium alloys: A review, *J. Nucl. Mater.* 518 (2019) 440–460, <https://doi.org/10.1016/j.jnucmat.2019.02.042>.
- [10] Y.-J. Jia, W.-Z. Han, Mechanisms of hydride nucleation, growth, reorientation, and embrittlement in zirconium: A review, *Materials (basel)* 16 (2023) 2419, <https://doi.org/10.3390/ma16062419>.
- [11] M.P. Puls, *The effect of hydrogen and hydrides on the integrity of zirconium alloy components - hydride reorientation*, ANT International, Tollerred, Sweden, 2018.
- [12] M. Le Saux, J. Besson, S. Carassou, C. Poussard, X. Averyt, Behavior and failure of uniformly hydrided Zircaloy-4 fuel claddings between 25 °C and 480 °C under various stress states, including RIA loading conditions, *Eng. Fail. Anal.* 17 (3) (2010) 683–700, <https://doi.org/10.1016/j.engfailanal.2009.07.001>.
- [13] H.H. Hsu, L.W. Tsay, Fracture properties of hydrided Zircaloy-4 cladding in recrystallization and stress-relief anneal conditions, *J. Nucl. Mater.* 422 (1–3) (2012) 116–123, <https://doi.org/10.1016/j.jnucmat.2011.12.032>.
- [14] B.V. Cockeram, J.L. Hollenbeck, The role of stress-state on the deformation and fracture mechanism of hydrided and non-hydrided Zircaloy-4, *J. Nucl. Mater.* 467 (2015) 9–31, <https://doi.org/10.1016/j.jnucmat.2015.09.012>.
- [15] S. Caré, A. Zaoui, Cavitation at triple nodes in α -zirconium polycrystals, *Acta Mater.* 44 (4) (1996) 1323–1336, [https://doi.org/10.1016/1359-6454\(95\)00302-9](https://doi.org/10.1016/1359-6454(95)00302-9).
- [16] G. Bertolino, G. Meyer, J. Perez Ipiña, Effects of hydrogen content and temperature on fracture toughness of Zircaloy-4, *J. Nucl. Mater.* 320 (3) (2003) 272–279, [https://doi.org/10.1016/S0022-3115\(03\)00193-4](https://doi.org/10.1016/S0022-3115(03)00193-4).
- [17] B.V. Cockeram, K.S. Chan, In situ studies and modeling of the deformation and fracture mechanism for wrought Zircaloy-4 and Zircaloy-2 as a function of stress-state, *J. Nucl. Mater.* 434 (1–3) (2013) 97–123, <https://doi.org/10.1016/j.jnucmat.2012.11.005>.
- [18] A. Zouari, M. Bono, D. Le Boulch, T. Le Jolu, J. Crépin, J. Besson, The effect of strain biaxiality on the fracture of zirconium alloy fuel cladding, *J. Nucl. Mater.* vol. 554 (May) (2021), <https://doi.org/10.1016/j.jnucmat.2021.153070>.
- [19] D. Setoyama, S. Yamanaka, Indentation creep study of zirconium hydrogen solid solution, *J. Alloys Compd.* 379 (1–2) (2004) 193–197, <https://doi.org/10.1016/j.jallcom.2004.02.035>.
- [20] R. Kishore, Effect of hydrogen on the creep behavior of Zr-2.5%Nb alloy at 723 K, *J. Nucl. Mater.* 385 (3) (2009) 591–594, <https://doi.org/10.1016/j.jnucmat.2009.01.034>.
- [21] F. Fagnoni, et al., Mechanical behavior of zircaloy-4 in the presence of hydrogen in solid solution at elevated temperatures, *Zircon. Nucl. Ind. 20th Int. Symp.* (2023) 218–235, <https://doi.org/10.1520/stp164520220019>.
- [22] F. Fagnoni, et al., Hydrogen enhanced localized plasticity in zirconium as observed by digital image correlation, *J. Nucl. Mater.* 590 (December) (2024) p. 154873, <https://doi.org/10.1016/j.jnucmat.2023.154873>.

- [23] Y. Il Jung, Y.N. Seol, B.K. Choi, J.Y. Park, Thermal creep of Zircaloy-4 tubes containing corrosion-induced hydrogen, *J. Nucl. Mater.* 419 (1–3) (2011) 213–216, <https://doi.org/10.1016/j.jnucmat.2011.08.047>.
- [24] D.S. Shih, I.M. Robertson, H.K. Birnbaum, Hydrogen embrittlement of α titanium: In situ TEM studies, *Acta Metall.* 36 (1) (1988) 111–124, [https://doi.org/10.1016/0001-6160\(88\)90032-6](https://doi.org/10.1016/0001-6160(88)90032-6).
- [25] L. Huang, D. Chen, E. Ma, Quantitative tests revealing hydrogen enhanced dislocation motion in α -iron, *Nat. Mater.* (2023), <https://doi.org/10.1038/s41563-023-01537-w>.
- [26] C. Domain, R. Besson, A. Legris, Atomic-scale ab initio study of the Zr-H system: II. Interaction of H with plane defects and mechanical properties, *Acta Mater.* 52 (6) (2004) 1495–1502, <https://doi.org/10.1016/j.actamat.2003.11.031>.
- [27] R. Choubey, M.P. Puls, Crack initiation at long radial hydrides in Zr-2.5Nb pressure tube material at elevated temperatures, *Metall. Mater. Trans. A* 25 (5) (1994) 993–1004, <https://doi.org/10.1007/BF02652274>.
- [28] S. Arsene, J. Bai, P. Bompard, Hydride embrittlement and irradiation effects on the hoop mechanical properties of pressurized water reactor (PWR) and boiling-water reactor (BWR) ZIRCALOY cladding tubes: Part I. Hydride Embrittlement in stress-relieved annealed and recrystallized ZIRCAL, *Metall. Mater. Trans. A Phys. Metall. Mater. Sci.* vol. 34 (2003) 554–566, <https://doi.org/10.1007/s11661-003-0091-3>.
- [29] J.H. Huang, S.P. Huang, Effect of hydrogen contents on the mechanical properties of Zircaloy-4, *J. Nucl. Mater.* 208 (1–2) (1994) 166–179, [https://doi.org/10.1016/0022-3115\(94\)90208-9](https://doi.org/10.1016/0022-3115(94)90208-9).
- [30] J. Li, et al., Effect of hydride precipitation on the fatigue cracking behavior in a zirconium alloy cladding tube, *Int. J. Fatigue* 129 (2019) 105230, <https://doi.org/10.1016/j.ijfatigue.2019.105230>.
- [31] S. Arsene, J. Bai, P. Bompard, Hydride embrittlement and irradiation effects on the hoop mechanical properties of pressurized water reactor (PWR) and boiling-water reactor (BWR) ZIRCALOY cladding tubes: Part III. Mechanical behavior of hydride in stress-relieved annealed and recrystall, *Metall. Mater. Trans. A Phys. Metall. Mater. Sci.* vol. 34 (2003) 579–588, <https://doi.org/10.1007/s11661-003-0093-1>.
- [32] H.E. Weekes, et al., In situ micropillar deformation of hydrides in Zircaloy-4, *Acta Mater.* 92 (2015) 81–96, <https://doi.org/10.1016/j.actamat.2015.03.037>.
- [33] M.P. Puls, S.Q. Shi, J. Rabier, Experimental studies of mechanical properties of solid zirconium hydrides, *J. Nucl. Mater.* 336 (1) (2005) 73–80, <https://doi.org/10.1016/j.jnucmat.2004.08.016>.
- [34] H. Wang, J. Thomas, M. A. Okuniewski, and V. Tomar, “Constitutive modeling of δ -phase zircaloy hydride based on strain rate dependent nanoindentation and nano-scale impact dataset,” *Int. J. Plast.*, vol. 133, no. March, p. 102787, 2020, doi: 10.1016/j.ijplas.2020.102787.
- [35] M. Kerr, M.R. Daymond, R.A. Holt, J.D. Almer, Strain evolution of zirconium hydride embedded in a Zircaloy-2 matrix, *J. Nucl. Mater.* 380 (1–3) (2008) 70–75, <https://doi.org/10.1016/j.jnucmat.2008.07.004>.
- [36] M. Grange, J. Besson, E. Andrieu, Anisotropic behavior and rupture of hydrided ZIRCALOY-4 sheets, *Metall. Mater. Trans. A* 31 (3) (2000) 679–690, <https://doi.org/10.1007/s11661-000-0010-9>.
- [37] M.P. Puls, Fracture initiation at hydrides in zirconium, *Metall. Trans. A* 22 (10) (1991) 2327–2337, <https://doi.org/10.1007/BF02664999>.
- [38] M.P. Puls, The influence of hydride size and matrix strength on fracture initiation at hydrides in zirconium alloys, *Metall. Trans. A* 19 (6) (1988) 1507–1522, <https://doi.org/10.1007/BF02674025>.
- [39] L.A. Simpson, Criteria for fracture initiation at hydrides in zirconium-2. 5 Pct niobium alloy, *Metall. Trans. a, Phys. Metall. Mater. Sci.* 12A (1981) 2113–2124, <https://doi.org/10.1007/BF02644181>.
- [40] F. Yunchang, D.A. Koss, The influence of multiaxial states of stress on the hydrogen embrittlement of zirconium alloy sheet, *Metall. Trans. A* 16 (4) (1985) 675–681, <https://doi.org/10.1007/BF02814242>.
- [41] M.R. Warren, O.J. Beevers, The interrelationship between deformation and crack nucleation and propagation in zirconium containing hydride precipitates, *J. Nucl. Mater.* 26 (3) (1968) 273–284, [https://doi.org/10.1016/0022-3115\(68\)90101-3](https://doi.org/10.1016/0022-3115(68)90101-3).
- [42] K.G. Barraclough, C.J. Beevers, Some observations on the deformation characteristics of bulk polycrystalline zirconium hydrides - Part 1 The deformation and fracture of hydrides based on the δ -phase, *J. Mater. Sci.* 4 (6) (1969) 518–525, <https://doi.org/10.1007/BF00550212>.
- [43] L. Reali, S. El Chamaa, D.S. Balint, C.M. Davies, M.R. Wenman, Deformation and fracture of zirconium hydrides during the plastic straining of Zr-4, *MRS Adv.* 5 (11) (2020) 559–567, <https://doi.org/10.1557/adv.2020.145>.
- [44] L. Reali, M.R. Wenman, A.P. Sutton, D.S. Balint, Plasticity of zirconium hydrides: a coupled edge and screw discrete dislocation model, *J. Mech. Phys. Solids* 147 (2021) 104219, <https://doi.org/10.1016/j.jmps.2020.104219>.
- [45] R. Thomas, et al., The role of hydrides and precipitates on the strain localisation behaviour in a zirconium alloy, *Acta Mater.* vol. 261 (August) (2023) 119327, <https://doi.org/10.1016/j.actamat.2023.119327>.
- [46] S. Wang, F. Giuliani, T. Ben Britton, Slip-hydride interactions in Zircaloy-4: Multiscale mechanical testing and characterisation, *Acta Mater.* 200 (2020) 537–550, <https://doi.org/10.1016/j.actamat.2020.09.038>.
- [47] S. Wang, S. Kalácska, X. Maeder, J. Michler, F. Giuliani, T. Ben Britton, The effect of δ -hydride on the micromechanical deformation of a Zr alloy studied by in situ high angular resolution electron backscatter diffraction, *Scr. Mater.* 173 (2019) 101–105, <https://doi.org/10.1016/j.scriptamat.2019.08.006>.
- [48] J. Beevers, D.V. Edmonds, On the room temperature fracture of zirconium/hydrogen alloys, *J. Nucl. Mater.* 33 (1) (1969) 107–113, [https://doi.org/10.1016/0022-3115\(69\)90014-2](https://doi.org/10.1016/0022-3115(69)90014-2).
- [49] C.M. Silva, F. Ibrahim, E.G. Lindquist, J.W. McMurray, C.D. Bryan, Brittle nature and the related effects of zirconium hydrides in Zircaloy-4, *Mater. Sci. Eng. A* vol. 767 (July) (2019) 138396, <https://doi.org/10.1016/j.msea.2019.138396>.
- [50] J. Li, et al., Uncovering the hydride orientation-mediated hoop fatigue mechanism in a zirconium alloy cladding tube, *Int. J. Plast.* vol. 159 (May) (2022) 103440, <https://doi.org/10.1016/j.ijplas.2022.103440>.
- [51] Y. Zhang, H. Qi, X. Song, Expansion deformation behavior of zirconium alloy claddings with different hydrogen concentrations, *J. Nucl. Mater.* 554 (2021) 153082, <https://doi.org/10.1016/j.jnucmat.2021.153082>.
- [52] J.H. Kim, M.H. Lee, B.K. Choi, Y.H. Jeong, Effect of the hydrogen contents on the circumferential mechanical properties of zirconium alloy claddings, *J. Alloys Compd.* 431 (1–2) (2007) 155–161, <https://doi.org/10.1016/j.jallcom.2006.05.074>.
- [53] A. Glendening, D.A. Koss, A.T. Motta, O.N. Pierron, R.S. Daum, Failure of hydrided zircaloy-4 under equal-biaxial and plane-strain tensile deformation, *J. ASTM Int.* 2 (6) (2005) 399–414, <https://doi.org/10.1520/jai12441>.
- [54] A. Gopalan, et al., Effect of radial hydride on room temperature fracture toughness of Zr-2.5Nb pressure tube material, *J. Nucl. Mater.* 544 (2021) 152681, <https://doi.org/10.1016/j.jnucmat.2020.152681>.
- [55] J.H. Huang, C.S. Ho, Effect of hydrogen gas on the mechanical properties of a zirconium alloy, *Mater. Chem. Phys.* 38 (2) (1994) 138–145, [https://doi.org/10.1016/0254-0584\(94\)90003-5](https://doi.org/10.1016/0254-0584(94)90003-5).
- [56] H. Chan, S.G. Roberts, J. Gong, Micro-scale fracture experiments on zirconium hydrides and phase boundaries, *J. Nucl. Mater.* 475 (2016) 105–112, <https://doi.org/10.1016/j.jnucmat.2016.03.026>.
- [57] Y. Zhang, L. You, X. Li, J. Zhou, X. Song, In-situ investigation of the fatigue crack initiation and propagation behavior of Zircaloy-4 with different hydrogen contents at RT and 300 °C, *J. Nucl. Mater.* 532 (2020) 152065, <https://doi.org/10.1016/j.jnucmat.2020.152065>.
- [58] H.C. Chu, S.K. Wu, K.F. Chien, R.C. Kuo, Effect of radial hydrides on the axial and hoop mechanical properties of Zircaloy-4 cladding, *J. Nucl. Mater.* 362 (1) (2007) 93–103, <https://doi.org/10.1016/j.jnucmat.2006.11.008>.
- [59] H.H. Hsu, L.W. Tsay, Effect of hydride orientation on fracture toughness of Zircaloy-4 cladding, *J. Nucl. Mater.* 408 (1) (2011) 67–72, <https://doi.org/10.1016/j.jnucmat.2010.10.068>.
- [60] K.S. Chan, X. He, Y.M. Pan, Fracture resistance of a zirconium alloy with reoriented hydrides, *Metall. Mater. Trans. A Phys. Metall. Mater. Sci.* 46 (1) (2014) 58–71, <https://doi.org/10.1007/s11661-014-2225-1>.
- [61] S.J. Min, J.J. Won, K.T. Kim, Terminal cool-down temperature-dependent hydride reorientations in Zr-Nb Alloy claddings under dry storage conditions, *J. Nucl. Mater.* 448 (1–3) (2014) 172–183, <https://doi.org/10.1016/j.jnucmat.2014.02.007>.

- [62] S.I. Hong, K.W. Lee, K.T. Kim, Effect of the circumferential hydrides on the deformation and fracture of Zircaloy cladding tubes, *J. Nucl. Mater.* 303 (2–3) (2002) 169–176, [https://doi.org/10.1016/S0022-3115\(02\)00814-0](https://doi.org/10.1016/S0022-3115(02)00814-0).
- [63] K. Tomiyasu, T. Sugiyama, T. Fuketa, Influence of cladding-peripheral hydride on mechanical fuel failure under reactivity-initiated accident conditions, *J. Nucl. Sci. Technol.* 44 (5) (2007) 733–742, <https://doi.org/10.1080/18811248.2007.9711862>.
- [64] P.A. Raynaud, D.A. Koss, A.T. Motta, Crack growth in the through-thickness direction of hydrided thin-wall Zircaloy sheet, *J. Nucl. Mater.* 420 (1–3) (2012) 69–82, <https://doi.org/10.1016/j.jnucmat.2011.09.005>.
- [65] A. Pineau, A.A. Benzerga, T. Pardoen, Failure of metals I: Brittle and ductile fracture, *Acta Mater.* 107 (2016) 424–483, <https://doi.org/10.1016/j.actamat.2015.12.034>.
- [66] J. Faleskog, C.F. Shih, Micromechanics of coalescence - I. Synergistic effects of elasticity, plastic yielding and multi-size-scale voids, *J. Mech. Phys. Solids* 45 (1) (1997) 21–25, [https://doi.org/10.1016/S0022-5096\(96\)00078-6](https://doi.org/10.1016/S0022-5096(96)00078-6).
- [67] G.D. Fearnough, A. Cowan, The effect of hydrogen and strain rate on the 'ductile-brittle' behaviour of Zircaloy, *J. Nucl. Mater.* 22 (1967) 137–147, [https://doi.org/10.1016/0022-3115\(67\)90023-2](https://doi.org/10.1016/0022-3115(67)90023-2).
- [68] T. Kubo, Y. Kobayashi, H. Uchikoshi, Determination of fracture strength of δ -zirconium hydrides embedded in zirconium matrix at high temperatures, *J. Nucl. Mater.* 435 (1–3) (2013) 222–230, <https://doi.org/10.1016/j.jnucmat.2012.12.045>.
- [69] M.C. Billone, T.A. Burtseva, R.E. Einziger, Ductile-to-brittle transition temperature for high-burnup cladding alloys exposed to simulated drying-storage conditions, *J. Nucl. Mater.* 433 (1–3) (2013) 431–448, <https://doi.org/10.1016/j.jnucmat.2012.10.002>.
- [70] J.S. Kim, T.H. Kim, D.H. Kook, Y.S. Kim, Effects of hydride morphology on the embrittlement of Zircaloy-4 cladding, *J. Nucl. Mater.* 456 (2015) 235–245, <https://doi.org/10.1016/j.jnucmat.2014.09.025>.
- [71] R.K. Sharma, S. Sunil, B.K. Kumawat, R.N. Singh, A. Tewari, B.P. Kashyap, Influence of hydride orientation on fracture toughness of CWSR Zr-2.5% Nb pressure tube material between RT and 300 C, *J. Nucl. Mater.* 488 (2017) 231–244, <https://doi.org/10.1016/j.jnucmat.2017.03.025>.
- [72] J.S. Kim, H.A. Kim, S.Y. Kang, Y.S. Kim, Effects of hydride rim on the ductility of Zircaloy-4 cladding, *J. Nucl. Mater.* 523 (2019) 383–390, <https://doi.org/10.1016/j.jnucmat.2019.06.007>.
- [73] A.K. Bind, R.N. Singh, Effect of hydrogen isotopes on tensile and fracture properties of Zr–2.5Nb pressure tube material, *Int. J. Fract.* 227 (2) (2021) 193–204, <https://doi.org/10.1007/s10704-020-00506-7>.
- [74] A.K. Bind, G. Avinash, S. Sunil, R.K. Sharma, R.N. Singh, Effect of radial hydrides on fracture behavior of Zr-2.5Nb pressure tube material, *J. Nucl. Mater.* 588 (July) (2024) p. 154800, <https://doi.org/10.1016/j.jnucmat.2023.154800>.
- [75] R.K. Sharma, A.K. Bind, G. Avinash, R.N. Singh, A. Tewari, B.P. Kashyap, Effect of radial hydride fraction on fracture toughness of CWSR Zr-2.5%Nb pressure tube material between ambient and 300 °C temperatures, *J. Nucl. Mater.* 508 (2018) 546–555, <https://doi.org/10.1016/j.jnucmat.2018.06.003>.
- [76] J.B. Bai, C. Prioul, D. François, Hydride embrittlement in ZIRCALOY-4 plate: Part I. Influence of microstructure on the hydride embrittlement in ZIRCALOY-4 at 20 °C and 350 °C, *Metall. Mater. Trans. A* 25 (6) (1994) 1185–1197, <https://doi.org/10.1007/BF02652293>.
- [77] S. Kim, J.H. Kang, Y. Lee, Hydride embrittlement resistance of Zircaloy-4 and Zr-Nb alloy cladding tubes and its implications on spent fuel management, *J. Nucl. Mater.* vol. 559 (November) (2022) 153393, <https://doi.org/10.1016/j.jnucmat.2021.153393>.
- [78] M.A. Martín-Rengel, F.J. Gómez Sánchez, J. Ruiz-Hervías, L. Caballero, A. Valiente, Revisiting the method to obtain the mechanical properties of hydrided fuel cladding in the hoop direction, *J. Nucl. Mater.* 429 (1–3) (2012) 276–283, <https://doi.org/10.1016/j.jnucmat.2012.06.003>.
- [79] O.N. Pierron, D.A. Koss, A.T. Motta, K.S. Chan, The influence of hydride blisters on the fracture of Zircaloy-4, *J. Nucl. Mater.* 322 (1) (2003) 21–35, [https://doi.org/10.1016/S0022-3115\(03\)00299-X](https://doi.org/10.1016/S0022-3115(03)00299-X).
- [80] A.H. de Menibus, et al., Fracture of Zircaloy-4 cladding tubes with or without hydride blisters in uniaxial to plane strain conditions with standard and optimized expansion due to compression tests, *Mater. Sci. Eng. A* 604 (2014) 57–66, <https://doi.org/10.1016/j.msea.2014.02.075>.
- [81] H.H. Hsu, M.F. Chiang, Y.C. Chen, The influence of hydride on fracture toughness of recrystallized Zircaloy-4 cladding, *J. Nucl. Mater.* 447 (1–3) (2014) 56–62, <https://doi.org/10.1016/j.jnucmat.2013.12.028>.
- [82] R.S. Daum, S. Majumdar, Y. Liu, M.C. Billone, Radial-hydride embrittlement of high-burnup zircaloy-4 fuel cladding, *J. Nucl. Sci. Technol.* 43 (9) (2006) 1054–1067, <https://doi.org/10.1080/18811248.2006.9711195>.
- [83] J.M. Lee, H.A. Kim, D.H. Kook, Y.S. Kim, A study on the effects of hydrogen content and peak temperature on threshold stress for hydride reorientation in Zircaloy-4 cladding, *J. Nucl. Mater.* 509 (2018) 285–294, <https://doi.org/10.1016/j.jnucmat.2018.07.005>.
- [84] H.C. Chu, S.K. Wu, R.C. Kuo, Hydride reorientation in Zircaloy-4 cladding, *J. Nucl. Mater.* 373 (1–3) (2008) 319–327, <https://doi.org/10.1016/j.jnucmat.2007.06.012>.
- [85] M. Nakatsuka and S. Yagnik, "Effect of Hydrides on Mechanical Properties and Failure Morphology of BWR Fuel Cladding at Very High Strain Rate," *J. ASTM Int.*, vol. 8, no. 1, p. Paper ID JA102954, 2010, doi: 10.1520/JA102954.
- [86] M.R. Louthan, R.P. Marshall, Control of hydride orientation in zircaloy, *J. Nucl. Mater.* 9 (2) (1963) 170–184, [https://doi.org/10.1016/0022-3115\(63\)90132-6](https://doi.org/10.1016/0022-3115(63)90132-6).
- [87] M. Aomi, et al., Evaluation of hydride reorientation behavior and mechanical properties for high-burnup fuel-cladding tubes in interim dry storage, *J. ASTM Int.* 5 (9) (2008) 651–673, <https://doi.org/10.1520/JA1101262>.
- [88] A. Yamauchi, K. Ogata, A study on macroscopic fuel cladding ductile-to-brittle transition at 300°C induced by radial hydrides, *J. Nucl. Sci. Technol.* 57 (3) (2020) 301–311, <https://doi.org/10.1080/00223131.2019.1676835>.
- [89] Q. Auzoux, et al., Hydride reorientation and its impact on mechanical properties of high burn-up and unirradiated cold-worked stress-relieved Zircaloy-4 and ZirloTM fuel cladding, *J. Nucl. Mater.* 494 (2022) 153893, <https://doi.org/10.1016/j.jnucmat.2022.153893>.
- [90] F. Nagase, T. Fuketa, Influence of hydride re-orientation on bwr cladding rupture under accidental conditions, *J. Nucl. Sci. Technol.* 41 (12) (2004) 1211–1217, <https://doi.org/10.1080/18811248.2004.9726350>.
- [91] S.I. Hong, K.W. Lee, Stress-induced reorientation of hydrides and mechanical properties of Zircaloy-4 cladding tubes, *J. Nucl. Mater.* 340 (2–3) (2005) 203–208, <https://doi.org/10.1016/j.jnucmat.2004.11.014>.
- [92] Y.J. Kim, D.H. Kook, T.H. Kim, J.S. Kim, Stress and temperature-dependent hydride reorientation of Zircaloy-4 cladding and its effect on the ductility degradation, *J. Nucl. Sci. Technol.* 52 (5) (2015) 717–727, <https://doi.org/10.1080/00223131.2014.978829>.
- [93] L. G. Bell and R. G. Duncan, "Hydride orientation in Zr-2.5% Nb; how it is affected by stress, temperature and heat treatment," Pinawa, Manitoba, Canada, 1975.
- [94] P.C.A. Simon, C. Frank, L.Q. Chen, M.R. Daymond, M.R. Tonks, A.T. Motta, Quantifying the effect of hydride microstructure on zirconium alloys embrittlement using image analysis, *J. Nucl. Mater.* 547 (2021) 152817, <https://doi.org/10.1016/j.jnucmat.2021.152817>.
- [95] S.Q. Shi, M.P. Puls, Criteria for fracture initiation at hydrides in zirconium alloys I. Sharp crack tip, *J. Nucl. Mater.* 208 (3) (1994) 232–242, [https://doi.org/10.1016/0022-3115\(94\)90332-8](https://doi.org/10.1016/0022-3115(94)90332-8).
- [96] T. Aliev, M. Kolesnik, Analytical approach to DHC description in zirconium alloys, *Int. J. Fract.* 228 (2021) 71–84, <https://doi.org/10.1007/s10704-021-00515-0>.
- [97] Q. Auzoux, et al., Hydride reorientation and its impact on ambient temperature mechanical properties of high burn-up irradiated and unirradiated recrystallized Zircaloy-2 nuclear fuel cladding with an inner liner, *J. Nucl. Mater.* 494 (2017) 114–126, <https://doi.org/10.1016/j.jnucmat.2017.07.022>.
- [98] K.N. Jang, K.T. Kim, The effect of neutron irradiation on hydride reorientation and mechanical property degradation of zirconium alloy cladding, *Nucl. Eng. Technol.* 49 (7) (2017) 1472–1482, <https://doi.org/10.1016/j.net.2017.05.006>.
- [99] S.Q. Shi, M.P. Puls, Fracture strength of hydride precipitates in Zr-2.5Nb alloys, *J. Nucl. Mater.* 275 (3) (1999) 312–317, [https://doi.org/10.1016/S0022-3115\(99\)00132-4](https://doi.org/10.1016/S0022-3115(99)00132-4).
- [100] R.N. Singh, H.K. Khandelwal, A.K. Bind, S. Sunil, P. Stähle, Influence of stress field of expanding and contracting plate shaped precipitate on hydride embrittlement of Zr-alloys, *Mater. Sci. Eng. A* 579 (2013) 157–163, <https://doi.org/10.1016/j.msea.2013.04.117>.

- [101] L.A. Simpson, C.D. Cann, Fracture toughness of zirconium hydride and its influence on the crack resistance of zirconium alloys, *J. Nucl. Mater.* 87 (1979) 303–316, [https://doi.org/10.1016/0022-3115\(79\)90567-1](https://doi.org/10.1016/0022-3115(79)90567-1).
- [102] L.J.S. Cherubin, F. Long, M. Topping, I.G.R. Santos, M.R. Daymond, Effect of Temperature and Irradiation on the Hardness of δ -Zr Hydride, *Zircon. Nucl. Ind. 20th Int. Symp.* (2023) 196–217, <https://doi.org/10.1520/stp164520220072>.
- [103] S. Ziaei, Q. Wu, M.A. Zikry, Orientation relationships between coherent interfaces in hcp-fcc systems subjected to high strain-rate deformation and fracture modes, *J. Mater. Res.* 30 (15) (2015) 2348–2359, <https://doi.org/10.1557/jmr.2015.207>.
- [104] S. Ziaei and M. A. Zikry, “How semi-coherent b.c.c. hydride interfacial interactions affect the inelastic deformation and fracture behavior of h.c.p. zirconium alloys,” *Mech. Mater.*, vol. 130, no. December 2018, pp. 1–8, 2019, doi: 10.1016/j.mechmat.2018.12.015.
- [105] T. Hasan, L. Capolungo, M.A. Zikry, How can machine learning be used for accurate representations and predictions of fracture nucleation in zirconium alloys with hydride populations? *APL Mater.* 11 (7) (2023) pp, <https://doi.org/10.1063/5.0155679>.
- [106] T. Hasan, L. Capolungo, M. Zikry, A machine learning microstructurally predictive framework for the failure of hydrided zirconium alloys, *Npj Mater. Degrad.* 7 (1) (2023) pp, <https://doi.org/10.1038/s41529-023-00344-7>.
- [107] T. Hasan, L. Capolungo, M.A. Zikry, Predictive machine learning approaches for the microstructural behavior of multiphase zirconium alloys, *Sci. Rep.* 13 (1) (2023) 5394, <https://doi.org/10.1038/s41598-023-32582-9>.
- [108] H. Tummala, L. Capolungo, C. Tomé, Quantifying the Stress State in the Vicinity of a δ -Hydride in α -Zirconium, *J. Nucl. Mater.* 511 (2018) 406–416, <https://doi.org/10.1016/j.jnucmat.2018.08.050>.
- [109] H. Ghaffarian, D. Jang, Deformation mechanism of embedded hydride within the polycrystalline zirconium matrix, *J. Nucl. Mater.* 565 (2022) 153736, <https://doi.org/10.1016/j.jnucmat.2022.153736>.
- [110] L. Reali, D.S. Balint, M.R. Wenman, Dislocation modelling of the plastic relaxation and thermal ratcheting induced by zirconium hydride precipitation, *J. Mech. Phys. Solids* 167 (June) (2022), <https://doi.org/10.1016/j.jmps.2022.104988>.
- [111] L. Reali, D.S. Balint, M.R. Wenman, Discrete dislocation modelling of δ hydrides in Zr: towards an understanding of the importance of interfacial stresses for crack initiation, *J. Nucl. Mater.* 572 (2022) 154091, <https://doi.org/10.1016/j.jnucmat.2022.154091>.
- [112] C.C. Tseng, M.H. Sun, C.K. Chao, Hydride effect on crack instability of Zircaloy cladding, *Nucl. Eng. Des.* 270 (2014) 427–435, <https://doi.org/10.1016/j.nucengdes.2014.01.013>.
- [113] M. Resta Levi and M. P. Puls, “DHC behaviour of irradiated Zr-2.5Nb pressure tubes up to 365C,” in *18th International Conference on Structural Mechanics in Reactor Technology (SMIRT 18)*, 2005, no. SMIRT 18, pp. 1811–1823.
- [114] K.S. Chan, A fracture model for hydride-induced embrittlement, *Acta Metall. Mater.* 43 (12) (1995) 4325–4335, [https://doi.org/10.1016/0956-7151\(95\)00133-G](https://doi.org/10.1016/0956-7151(95)00133-G).
- [115] K.F. Nilsson, N. Jakšić, V. Vokál, An elasto-plastic fracture mechanics based model for assessment of hydride embrittlement in zircaloy cladding tubes, *J. Nucl. Mater.* 396 (1) (2010) 71–85, <https://doi.org/10.1016/j.jnucmat.2009.10.056>.
- [116] W. Qin, J.A. Szpunar, J. Kozinski, Hydride-induced degradation of zirconium alloys: A criterion for complete ductile-to-brittle transition and its dependence on microstructure, *Proc. R. Soc. A Math. Phys. Eng. Sci.* 471 (2182) (2015) pp, <https://doi.org/10.1098/rspa.2015.0192>.
- [117] R. Liu, A. Mostafa, Z. Liu, Modeling of structural failure of Zircaloy claddings induced by multiple hydride cracks, *Int. J. Fract.* 213 (2) (2018) 171–191, <https://doi.org/10.1007/s10704-018-0312-9>.
- [118] W. Qin, J.A. Szpunar, N.A.P. Kiran Kumar, J. Kozinski, Microstructural criteria for abrupt ductile-to-brittle transition induced by δ -hydrides in zirconium alloys, *Acta Mater.* 81 (2014) 219–229, <https://doi.org/10.1016/j.actamat.2014.08.010>.
- [119] K. Une, K. Nogita, S. Ishimoto, K. Ogata, Crystallography of zirconium hydrides in recrystallized zircaloy-2 fuel cladding by electron backscatter diffraction, *J. Nucl. Sci. Technol.* 41 (7) (2004) 731–740, <https://doi.org/10.1080/18811248.2004.9715540>.
- [120] M. Veleva, S. Arsene, M.C. Record, J.L. Bechade, J. Bai, Hydride embrittlement and irradiation effects on the hoop mechanical properties of pressurized water reactor (PWR) and boiling-water reactor (BWR) ZIRCALOY cladding tubes: Part II. Morphology of hydrides investigated at different magnifications and their, *Metall. Mater. Trans. A Phys. Metall. Mater. Sci.* vol. 34 (2003) 567–578, <https://doi.org/10.1007/s11661-003-0092-2>.
- [121] G.M. Han, et al., Phase-field modeling of stacking structure formation and transition of δ -hydride precipitates in zirconium, *Acta Mater.* 165 (2019) 528–546, <https://doi.org/10.1016/j.actamat.2018.12.009>.
- [122] T.W. Heo, K.B. Colas, A.T. Motta, L.Q. Chen, A phase-field model for hydride formation in polycrystalline metals: Application to δ -hydride in zirconium alloys, *Acta Mater.* 181 (2019) 262–277, <https://doi.org/10.1016/j.actamat.2019.09.047>.
- [123] P.C.A. Simon, et al., Investigation of δ zirconium hydride morphology in a single crystal using quantitative phase field simulations supported by experiments, *J. Nucl. Mater.* 557 (2021) 153303, <https://doi.org/10.1016/j.jnucmat.2021.153303>.
- [124] V.O. Kharchenko, X. Kong, T. Xin, L. Wu, O.M. Shchokotova, Phase field modeling of precipitation in Zr-1%Nb-1%Sn alloy: a study of statistical properties and mechanical response, *Phys. Scr.* 98 (2023) 035714, <https://doi.org/10.1088/1402-4896/acbcf9>.
- [125] N.A.P. Kiran Kumar, Hydride formation in zirconium alloys, McGill University, 2011.
- [126] A. Toghraee, J. Bair, M.A. Zaeem, Effects of applied strain on formation, shape evolution, and reorientation of multiphase zirconium hydrides: A multiphase field modeling study, *Comput. Mater. Sci.* 192 (2021) 110367, <https://doi.org/10.1016/j.commatsci.2021.110367>.
- [127] W. Qin, et al., Threshold stress of hydride reorientation in zirconium alloy nuclear fuel cladding tubes: A theoretical determination, *J. Nucl. Mater.* 563 (2022), <https://doi.org/10.1016/j.jnucmat.2022.153659>.
- [128] C.E. Ells, The stress orientation of hydride in zirconium alloys, *J. Nucl. Mater.* 35 (3) (1970) 306–315, [https://doi.org/10.1016/0022-3115\(70\)90214-X](https://doi.org/10.1016/0022-3115(70)90214-X).
- [129] D. Hardie, M.W. Shanahan, Stress reorientation of hydrides in zirconium-2.5% niobium, *J. Nucl. Mater.* 55 (1) (1975) 1–13, [https://doi.org/10.1016/0022-3115\(75\)90132-4](https://doi.org/10.1016/0022-3115(75)90132-4).
- [130] J.B. Bai, N. Ji, D. Gilbon, C. Prioul, D. François, Hydride embrittlement in ZIRCALOY-4 plate: Part II. interaction between the tensile stress and the hydride morphology, *Metall. Mater. Trans. A* 25 (6) (1994) 1199–1208, <https://doi.org/10.1007/BF02652294>.
- [131] M.P. Puls, Effects of misfit and external stresses on terminal solid solubility in hydride-forming metals, *Acta Metall.* 29 (12) (1981) 1961–1968, [https://doi.org/10.1016/0001-6160\(81\)90033-x](https://doi.org/10.1016/0001-6160(81)90033-x).
- [132] J.Y.R. Rashid, A.J. Machiels, Hydride precipitation in spent fuel cladding during storage. *The 10th International Conference on Environmental Remediation and Radioactive Waste Management, ICEM05-1038*, 2005.
- [133] J. Rashid and A. Machiels, “Threat of hydride re-orientation to spent fuel integrity during transportation accidents: Myth or reality?,” *Am. Nucl. Soc. - 2007 LWR Fuel Performance/Top Fuel*, pp. 464–471, 2007.
- [134] A.R. Massih, L.O. Jernkvist, Stress orientation of second-phase in alloys: Hydrides in zirconium alloys, *Comput. Mater. Sci.* 46 (4) (2009) 1091–1097, <https://doi.org/10.1016/j.commatsci.2009.05.025>.
- [135] M. Kolesnik, T. Aliev, V. Likhanskii, Modeling of hydrogen behavior in spent fuel claddings during dry storage, *J. Nucl. Mater.* 508 (2018) 567–573, <https://doi.org/10.1016/j.jnucmat.2018.06.012>.
- [136] T. Aliev, M. Kolesnik, V. Likhanskii, V. Saiutina, Modeling of hydride reorientation in E110 during thermal cycling, *J. Nucl. Mater.* 557 (2021) 153230, <https://doi.org/10.1016/j.jnucmat.2021.153230>.
- [137] F. Feria, C. Aguado, L.E. Herranz, Extension of FRAPCON-xt to hydride radial reorientation in dry storage, *Ann. Nucl. Energy* 145 (2020) 107559, <https://doi.org/10.1016/j.anucene.2020.107559>.
- [138] K.S. Chan, A micromechanical model for predicting hydride embrittlement in nuclear fuel cladding material, *J. Nucl. Mater.* 227 (3) (1996) 220–236, [https://doi.org/10.1016/0022-3115\(95\)00160-3](https://doi.org/10.1016/0022-3115(95)00160-3).
- [139] M. Kolesnik, T. Aliev, V. Likhanskii, Modeling of size, aspect ratio, and orientation of flattened precipitates in the context of Zr-H system under external stress, *Comput. Mater. Sci.* 189 (2021) 110260, <https://doi.org/10.1016/j.commatsci.2020.110260>.
- [140] M. Kolesnik, T. Aliev, Evaluating the spatial and size distributions of flat precipitates in diffusion-controlled precipitation processes, *Phys. Met. Metallogr.* 104 (2023), <https://doi.org/10.1134/S0031918X22602074>.

- [141] T. Aliev, M. Kolesnik, Evolution of an approach to the modeling of zirconium hydrides morphology based on Monte-Carlo method in 3D representation, *Lett. Mater.* 13 (2) (2023) 143–148.
- [142] J.R. Rice, D.M. Tracey, On the ductile enlargement of voids in triaxial stress fields, *J. Mech. Phys. Solids* 17 (3) (1969) 201–217, [https://doi.org/10.1016/0022-5096\(69\)90033-7](https://doi.org/10.1016/0022-5096(69)90033-7).
- [143] B.V. Cockeram, K.S. Chan, In situ studies and modeling the fracture of Zircaloy-4, *J. Nucl. Mater.* 393 (3) (2009) 387–408, <https://doi.org/10.1016/j.jnucmat.2009.06.033>.
- [144] J.W. Hutchinson, Singular behaviour at the end of a tensile crack in a hardening material, *J. Mech. Phys. Solids* 16 (1968) 13–31.
- [145] J.R. Rice, G.F. Rosengren, Plane strain deformation near a crack tip in a power-law hardening material, *J. Mech. Phys. Solids* 16 (1) (1968) 1–12, [https://doi.org/10.1016/0022-5096\(68\)90013-6](https://doi.org/10.1016/0022-5096(68)90013-6).
- [146] A.L. Gurson, Continuum theory of ductile rupture by void nucleation and growth: Part I - yield criteria and flow rules for porous ductile media, *J. Eng. Mater. Technol.* 99 (1977) 2–15.
- [147] V. Tvergaard, A. Needleman, Analysis of the cup-cone fracture in a round tensile bar, *Acta Metall.* 32 (1) (1984) 157–169, [https://doi.org/10.1016/0001-6160\(84\)90213-X](https://doi.org/10.1016/0001-6160(84)90213-X).
- [148] B.W. Williams, S. St Lawrence, B.W. Leitch, Comparison of the measured and predicted crack propagation behaviour of Zr-2.5Nb pressure tube material, *Eng. Fract. Mech.* 78 (18) (2011) 3135–3152, <https://doi.org/10.1016/j.engfracmech.2011.06.020>.
- [149] J. Zhou, X. Gao, J.C. Sobotka, B.A. Webler, B.V. Cockeram, On the extension of the Gurson-type porous plasticity models for prediction of ductile fracture under shear-dominated conditions, *Int. J. Solids Struct.* 51 (18) (2014) 3273–3291, <https://doi.org/10.1016/j.ijsolstr.2014.05.028>.
- [150] F. Prat, M. Grange, J. Besson, E. Andrieu, Behavior and rupture of hydrided Zircaloy-4 tubes and sheets, *Metall. Mater. Trans. A* 29 (1998) 1643–1651, <https://doi.org/10.1007/s11661-998-0087-0>.
- [151] M. Grange, J. Besson, E. Andrieu, An anisotropic Gurson type model to represent the ductile rupture of hydrided Zircaloy-4 sheets, *Int. J. Fract.* 105 (3) (2000) 273–293, <https://doi.org/10.1023/A:1007615513884>.
- [152] M. Le Saux, J. Besson, S. Carassou, A model to describe the mechanical behavior and the ductile failure of hydrided Zircaloy-4 fuel claddings between 25°C and 480°C, *J. Nucl. Mater.* 466 (2015) 43–55, <https://doi.org/10.1016/j.jnucmat.2015.07.026>.
- [153] D.S. Dugdale, Yielding of steel sheets containing slits, *J. Mech. Phys. Solids* 8 (1960) 100–104, <https://doi.org/10.12989/cac.2015.15.5.735>.
- [154] G.I. Barenblatt, The mathematical theory of equilibrium cracks in brittle fracture, *Adv. Appl. Mech.* 7 (1962) 55–129.
- [155] A. Hillerborg, M. Modéer, P.E. Petersson, Analysis of crack formation and crack growth in concrete by means of fracture mechanics and finite elements, *Cem. Concr. Res.* 6 (1976) 773–782.
- [156] A. Needleman, Continuum model for void nucleation by inclusion debonding, *Am. Soc. Mech. Eng.* 54 (1987) 525–531.
- [157] A. Corneil, I. Scheider, K.H. Schwalbe, On the practical application of the cohesive model, *Eng. Fract. Mech.* 70 (14) (2003) 1963–1987, [https://doi.org/10.1016/S0013-7944\(03\)00134-6](https://doi.org/10.1016/S0013-7944(03)00134-6).
- [158] D. Wäßling, A.R. Massih, P. Stähle, A model for hydride-induced embrittlement in zirconium-based alloys, *J. Nucl. Mater.* 249 (2–3) (1997) 231–238, [https://doi.org/10.1016/S0022-3115\(97\)00183-9](https://doi.org/10.1016/S0022-3115(97)00183-9).
- [159] Y.S. Kim, Y.G. Matvienko, Y.M. Cheong, S.S. Kim, S.C. Kwon, Model of the threshold stress intensity factor, K_{IH}, for delayed hydride cracking of Zr-2.5Nb alloy, *J. Nucl. Mater.* 278 (2) (2000) 251–257, [https://doi.org/10.1016/S0022-3115\(99\)00249-4](https://doi.org/10.1016/S0022-3115(99)00249-4).
- [160] Y.G. Matvienko, The cohesive zone model in a problem of delayed hydride cracking of zirconium alloys, *Int. J. Fract.* 128 (1) (2004) 73–79, <https://doi.org/10.1023/B:FRAC.0000040969.02493.09>.
- [161] A. Banerjee, R. Manivasagam, Triaxiality dependent cohesive zone model, *Eng. Fract. Mech.* 76 (12) (2009) 1761–1770, <https://doi.org/10.1016/j.engfracmech.2009.03.009>.
- [162] C. Fang, X. Guo, G.J. Weng, J.H. Li, G. Chen, Simulation of ductile fracture of zirconium alloys based on triaxiality dependent cohesive zone model, *Acta Mechanica* 232 (9) (2021) 3723–3736, <https://doi.org/10.1007/s00707-021-03032-2>.
- [163] W. Chen, H. Kou, L. Chen, F. Wang, X. Zeng, Theory model combined with XFEM of threshold stress intensity factor and critical hydride length for delay hydride cracking, *Int. J. Hydrogen Energy* 44 (54) (2019) 29047–29056, <https://doi.org/10.1016/j.ijhydene.2019.08.157>.
- [164] C. Fang, X. Guo, J. Li, G. Chen, Relations of microstructural attributes and strength - ductility of zirconium alloys with hydrides, *Chinese J. Mech. Eng.* (2023), <https://doi.org/10.1186/s10033-023-00925-2>.
- [165] Q. Chen, J.T. Ostien, G. Hansen, Development of a used fuel cladding damage model incorporating circumferential and radial hydride responses, *J. Nucl. Mater.* 447 (1–3) (2014) 292–303, <https://doi.org/10.1016/j.jnucmat.2014.01.001>.
- [166] S.S. Kulkarni, V. Gupta, D. Senor, T. Truster, A. Soulami, R. Devanathan, A microstructure-based modeling approach to predict the mechanical properties of Zr alloy with hydride precipitates, *Comput. Mater. Sci.* vol. 197 (May) (2021) 110654, <https://doi.org/10.1016/j.commatsci.2021.110654>.
- [167] S. El Chamaa, M. Patel, C.M. Davies, M.R. Wenman, The Effect of Grain Boundaries and Second-Phase Particles on Hydride Precipitation in Zirconium Alloys, *MRS Adv.* 3 (31) (2018) 1749–1754, <https://doi.org/10.1557/adv.2018.111>.
- [168] R.N. Singh, et al., Effect of direction of approach of test temperature on fracture toughness of Zr-2.5Nb pressure tube material, *Mater. Sci. Eng. A* 621 (2015) 190–197, <https://doi.org/10.1016/j.msea.2014.10.052>.
- [169] O. Zanellato, et al., Synchrotron diffraction study of dissolution and precipitation kinetics of hydrides in Zircaloy-4, *J. Nucl. Mater.* 420 (1–3) (2012) 537–547, <https://doi.org/10.1016/j.jnucmat.2011.11.009>.